Chapter 5
Time Response-Based Design

Consider the closed-loop system in Fig. 5.1. In Example 4.3, Sect. 4.1, it is shown that the closed-loop transfer function is given as:

$$M(s) = \frac{C(s)}{R(s)} = \frac{G(s)}{1 + G(s)H(s)}. \tag{5.1}$$

In Chap. 3 it is explained that the time response $c(t) = \mathcal{L}^{-1}\{C(s)\} = \mathcal{L}^{-1}\{M(s)R(s)\}$ is given as the addition of the natural response and the forced response: $c(t) = c_n(t)+c_f(t)$. The objectives of the control system in Fig. 5.1 are:

- The closed-loop control system is stable, i.e., $\lim_{t\to\infty} c_n(t) = 0$, which is ensured if all of poles of the closed-loop transfer function $M(s)$ have a negative real part. This is important because it ensures that $c(t) \to c_f(t)$ as time increases.
- The convergence $c_n(t) \to 0$ is fast.
- The forced response is equal to the desired output $c_f(t) = r(t) = \mathcal{L}^{-1}\{R(s)\}$.

The last item constitutes the specifications of the response in a steady state and the way to ensure this is studied in Sect. 4.4. The second item constitutes the transient response specifications and the way to satisfy them is studied in the current chapter. It must be stressed that ensuring the desired transient response specifications must also ensure closed-loop stability.

The design of a controller is performed by suitably assigning the poles (the roots of $1 + G(s)H(s)$) and the zeros (the roots of $G(s)$) of the closed-loop transfer function $M(s)$. In classical control, the plant poles and zeros are always assumed to be known, whereas the structure of the controller is proposed to satisfy the steady-state response specifications, for instance. However, the exact location of the poles and zeros of the controller must be selected to ensure that the closed-loop poles, i.e., the roots of $1 + G(s)H(s)$, are placed at the desired values and that the closed-

V. M. Hernández-Guzmán, R. Silva-Ortigoza, *Automatic Control with Experiments*,
Advanced Textbooks in Control and Signal Processing,
https://doi.org/10.1007/978-3-319-75804-6_5

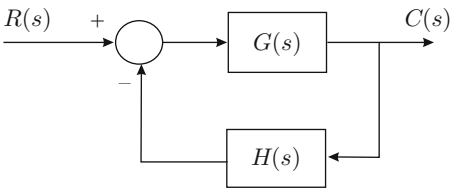

Fig. 5.1 Closed-loop system

loop zeros, i.e., $G(s) = 0$, are also suitably located.[1] In this chapter, one of the main classical control techniques for control design is studied: *the root locus method* (see [1] for a historical perspective). This method assigns poles of the closed-loop transfer function $M(s)$ through a suitable modification of the *open-loop transfer function* $G(s)H(s)$. Moreover, it is also possible to place the zeros of the closed-loop transfer function $M(s)$ such that their effects on the closed-loop system response are small.

5.1 Drawing the Root Locus Diagram

Assuming that the poles and zeros of the plant are known, the root locus method is a graphical tool that is useful to locate the closed-loop poles by suitably selecting poles and zeros of a controller. Moreover, this can also be performed by cancelling some undesired (slow) closed-loop poles with some controller zeros. According to Sect. 3.5.1, this achieves system order reduction and the elimination of some zeros such that the closed-loop system transient response can be approximated by some of the simple cases studied in Sects. 3.1.1 and 3.3.1. This simplifies the task of designing a controller such that the closed-loop transfer function $M(s)$ has poles and zeros that ensure the desired transient response specifications.

The root locus diagram is represented by several curves whose points constitute the closed-loop system poles parameterized by the open loop-gain, k, which takes values from $k = 0$ to $k = +\infty$. According to (5.1), every closed-loop pole s, i.e., a point in the s plane belonging to the root locus, must satisfy $1 + G(s)H(s) = 0$. The root locus diagram is drawn by proposing points s on the complex plane s, which are checked to satisfy $1 + G(s)H(s) = 0$. To verify this condition in a simple manner, a set of rules are proposed, which are listed next. Following these rules, the root locus diagram is drawn using the poles and zeros of the open-loop transfer function $G(s)H(s)$ as data. This means that the closed-loop poles are determined by the open-loop poles and zeros.

It is assumed that the open-loop transfer function can be written as:

$$G(s)H(s) = k\frac{\prod_{j=1}^{m}(s - z_j)}{\prod_{i=1}^{n}(s - p_i)}, \quad n > m, \tag{5.2}$$

[1] Although the poles determine stability and transient response, zeros also have an effect on the final shape of the transient response (see Sect. 8.1, Chap. 8). This is the reason why the design based on the root locus is sometimes performed by trying to cancel one closed-loop pole with a closed-loop zero.

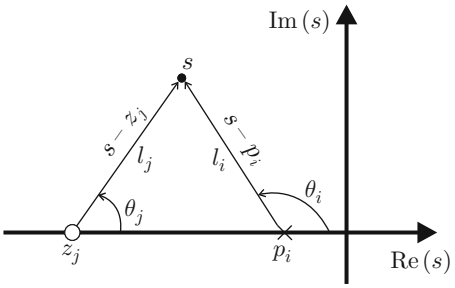

Fig. 5.2 Graphical representation of factors $s - z_j$ and $s - p_i$

where z_j, $j = 1, \ldots, m$, are the open-loop zeros and p_i, $i = 1, \ldots, n$, are the open-loop poles. As z_j, p_i and s are, in general, complex numbers located on the s plane, the following can be written:

$$s - z_j = l_j \angle \theta_j,$$
$$s - p_i = l_i \angle \theta_i,$$

as depicted in Fig. 5.2. Then:

$$G(s)H(s) = k\frac{\prod_{j=1}^{m} l_j \angle \theta_j}{\prod_{i=1}^{n} l_i \angle \theta_i} = k\frac{\prod_{j=1}^{m} l_j}{\prod_{i=1}^{n} l_i} \angle \left(\sum_{j=1}^{m} \theta_j - \sum_{i=1}^{n} \theta_i \right). \tag{5.3}$$

On the other hand, the closed-loop poles are those values of s satisfying the following:

$$1 + G(s)H(s) = 0. \tag{5.4}$$

This means that closed-loop poles are those values of s satisfying:

$$G(s)H(s) = -1 = 1\angle \pm (2q+1)180^\circ, \quad q = 0, 1, 2, \ldots \tag{5.5}$$

Using (5.3) and (5.5) the so-called *magnitude condition* (5.6) and *angle condition* (5.7) are obtained, which must be satisfied by every closed-loop pole s, i.e., those points s belonging to root locus:

$$k\frac{\prod_{j=1}^{m} l_j}{\prod_{i=1}^{n} l_i} = 1, \tag{5.6}$$

$$\sum_{j=1}^{m} \theta_j - \sum_{i=1}^{n} \theta_i = \pm(2q+1)180^\circ, \quad q = 0, 1, 2, \ldots \tag{5.7}$$

From these conditions, the following rules are obtained [6–9].

5.1.1 Rules for Drawing the Root Locus Diagram

1. **The root locus starts ($k = 0$) at the open-loop poles.**
   Using (5.2) and (5.4):

$$\begin{aligned} 1 + G(s)H(s) &= 1 + k\frac{\prod_{j=1}^{m}(s - z_j)}{\prod_{i=1}^{n}(s - p_i)} = 0, \\ &= \frac{\prod_{i=1}^{n}(s - p_i) + k\prod_{j=1}^{m}(s - z_j)}{\prod_{i=1}^{n}(s - p_i)} = 0, \\ &= \prod_{i=1}^{n}(s - p_i) + k\prod_{j=1}^{m}(s - z_j) = 0, \\ &= \prod_{i=1}^{n}(s - p_i) = 0, \end{aligned} \tag{5.8}$$

   if $k = 0$. This means that the closed-loop poles (those that satisfy $1 + G(s)H(s) = 0$) are identical to the open-loop poles ($s = p_i, i = 1, \ldots, n$) if $k = 0$.
2. **Root locus ends ($k \to \infty$) at the open-loop zeros.**
   From (5.8):

$$\begin{aligned} 1 + G(s)H(s) &= \prod_{i=1}^{n}(s - p_i) + k\prod_{j=1}^{m}(s - z_j) = 0, \\ &\approx k\prod_{j=1}^{m}(s - z_j) = 0, \end{aligned}$$

   because $\prod_{i=1}^{n}(s-p_i) \ll k\prod_{j=1}^{m}(s-z_j)$ if $k \to \infty$. This means that the closed-loop poles (those satisfying $1 + G(s)H(s) = 0$) are identical to the open-loop zeros ($s = z_j, j = 1, \ldots, m$) when $k \to \infty$.
3. **When $k \to \infty$ there are $n - m$ branches of the root locus that tend toward some point at the infinity of the plane s. This means that the open-loop transfer function $G(s)H(s)$ has $n - m$ zeros at infinity.**
   These branches can be identified by the angle of the asymptote where the root locus diagram approaches as $k \to \infty$. The angle that each asymptote forms with the positive real axis can be computed as:

$$\text{asymptote angle} = \frac{\pm 180°(2q + 1)}{n - m}, \quad q = 0, 1, 2, \ldots \tag{5.9}$$

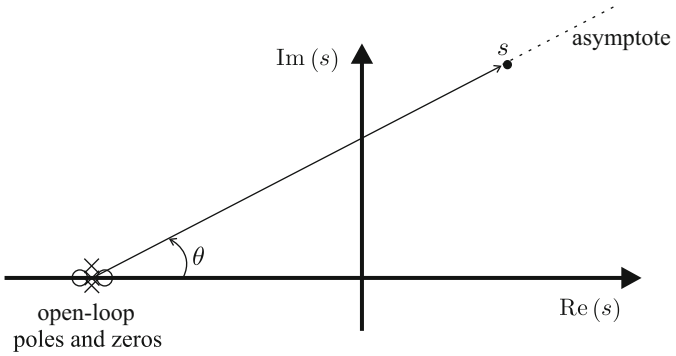

Fig. 5.3 Asymptote angle in rule 3

This formula is obtained as follows. Consider a point s that belongs to an asymptote and is located far away from the origin. Hence, all poles and zeros of $G(s)H(s)$, are observed as gathered in a single point of the plane s, as depicted in Fig. 5.3. Thus, the angle contributed by each open-loop pole and zero to the condition in (5.7) (see Fig. 5.3) is identical to the angle contributed by the others, i.e., representing such an angle by θ, the angle condition (5.7) can be written as:

$$\sum_{j=1}^{m} \theta_j - \sum_{i=1}^{n} \theta_i = (m-n)\theta = \pm(2q+1)180^\circ, \quad q = 0, 1, 2, \ldots$$

Solving this expression for θ yields:

$$\theta = \frac{\pm(2q+1)180^\circ}{n-m}, \quad q = 0, 1, 2, \ldots$$

which becomes (5.9) when θ =asymptote angle (see Fig. 5.3).

4. **Point σ_a where asymptotes intersect the real axis is computed as [5], Chap. 6:**

$$\sigma_a = \frac{\sum_i p_i - \sum_j z_j}{n-m}.$$

5. **Consider a point on the real axis of the plane s. Suppose that the number of real open-loop poles plus the number of real open-loop zeros on the right of such a point is equal to an odd number. Then such a point on the real axis belongs to the root locus. If this is not the case, then such a point does not belong to the root locus.**

Observe Fig. 5.4 and recall the angle condition (5.7). Notice that two open-loop complex conjugate poles or zeros produce angles that added to result in 0° or 360° and, hence, have no contribution to the angle condition (5.7). This means that, in this rule, only real open-loop poles and zeros must be considered in (5.7). On the other hand, notice that any real pole or zero located at the left of the test point s contributes with a zero angle. This means that, in this rule, in the expression (5.7), only real open-loop poles and zeros located on the right of the test point s must be considered. Notice that each real open-loop zero on the right of the point s contributes with a $+180°$ angle, whereas each real open-loop pole at the right of the same point contributes with a $-180°$ angle. Hence, the total angle contributed by all open-loop poles and zeros appearing on the right of the test point s is:

$$\sum_{j=1}^{m} \theta_j - \sum_{i=1}^{n} \theta_i = m_1(+180°) + n_1(-180°),$$

where m_1 and n_1 stand for the number of real open-loop zeros and poles respectively, on the right of the test point s. On the other hand, if the subtraction of two numbers is equal to an odd number, then the addition of the same numbers is also an odd number. Hence, if:

$$\sum_{j=1}^{m} \theta_j - \sum_{i=1}^{n} \theta_i = (m_1 - n_1) \times (+180°) = \pm(2q+1)180°,$$

for some $q = 0, 1, 2, \ldots$, i.e., $m_1 - n_1$ is odd, then it is also true that:

$$\sum_{j=1}^{m} \theta_j - \sum_{i=1}^{n} \theta_j = (m_1 + n_1) \times (+180°) = \pm(2q+1)180°,$$

for some $q = 0, 1, 2, \ldots$, i.e., $m_1 + n_1$ is odd. Notice that this last expression constitutes the angle condition (5.7) and, thus, the test point s in Fig. 5.4 is a closed-loop pole and belongs to the root locus.

6. **The root locus is symmetrical with respect to the real axis.**
   This is easily understood by recalling that all complex poles appear simultaneously with their complex conjugate pair (see first paragraph in Sect. 3.4.3).
7. **The departure angle from an open-loop complex pole is computed as:**
   Departure angle from a complex pole=
   $\pm(2q+1)180° + \sum$[angles of vectors from the open-loop zeros to the open-loop pole under study]
   $-\sum$[angles of vectors from the other open-loop poles to the open-loop pole under study]

(5.10)

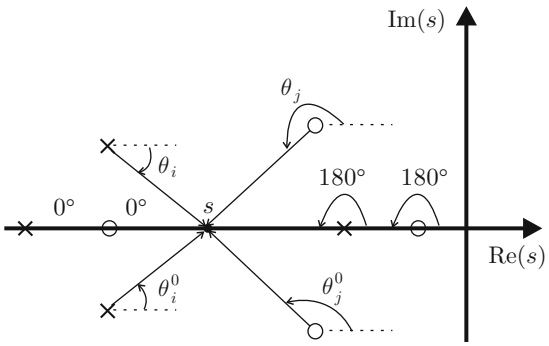

Fig. 5.4 Open-loop poles and zeros used to study rule 5

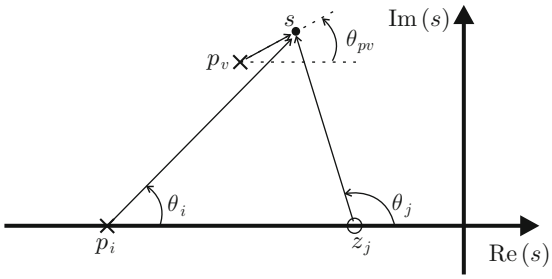

Fig. 5.5 Open-loop poles and zeros in the study of rule 7

Consider Fig. 5.5. Assume that the point s belongs to the root locus and it is very close to open-loop pole at p_v. The angle θ_{pv} is the departure angle from the open-loop complex pole at p_v. According to the angle condition (5.7):

$$\begin{aligned}&\sum_{j=1}^{m}\theta_j-\sum_{i=1}^{n}\theta_i=\\&=(\theta_{z1}+\theta_{z2}+\cdots+\theta_{zm})-(\theta_{p1}+\theta_{p2}+\cdots+\theta_{pv}+\cdots+\theta_{pn})\\&=\pm(2q+1)180^\circ,\quad q=0,1,2,\ldots\end{aligned}$$

where θ_{zj} and θ_{pi} stand for the angles due to the open-loop zeros and poles respectively. Solving for θ_{pv}:

$$\theta_{pv}=\pm(2q+1)180^\circ+(\theta_{z1}+\theta_{z2}+\cdots+\theta_{zm})-(\theta_{p1}+\theta_{p2}+\cdots+\theta_{pn}),$$

for $q=0,1,2,\ldots$, which is equivalent to (5.10) because $s=p_v$ can be assumed as they are very close.

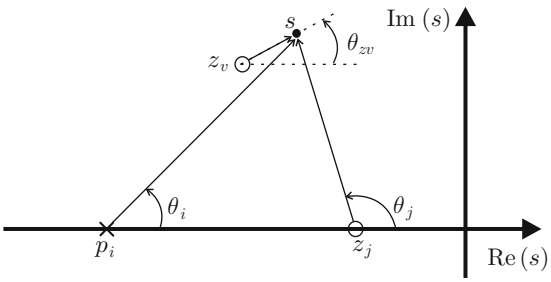

Fig. 5.6 Open-loop poles and zeros in the study of rule 8

8. **The arrival angle to an open-loop complex zero is computed as:**
Arrival angle to a complex zero=
$\pm(2q+1)180^\circ - \sum$[angles of vectors from the other open-loop zeros to the open-loop zero under study]
$+\sum$[angles of vectors from the open-loop poles to the open-loop zero under study]

(5.11)

Consider Fig. 5.6. Assume that the point s belongs to the root locus and is very close to zero at z_v. The angle θ_{zv} is the arrival angle to the open-loop zero at z_v. According to the angle condition (5.7):

$$\sum_{j=1}^{m}\theta_j - \sum_{i=1}^{n}\theta_i =$$
$$= (\theta_{z1}+\theta_{z2}+\cdots+\theta_{zv}+\cdots+\theta_{zm}) - (\theta_{p1}+\theta_{p2}+\cdots+\theta_{pn}),$$
$$= \pm(2q+1)180^\circ,$$

where $q = 0, 1, 2, \ldots$, whereas θ_{zj} and θ_{pi} stand for the angles due to the open-loop zeros and poles respectively. Solving for θ_{zv}:

$$\theta_{zv} = \pm(2q+1)180^\circ - (\theta_{z1}+\theta_{z2}+\cdots+\theta_{zm}) + (\theta_{p1}+\theta_{p2}+\cdots+\theta_{pn}),$$

for $q = 0, 1, 2, \ldots$, which is equivalent to (5.11) because $s = z_v$ can be assumed as they are very close.

9. **The open-loop gain, k, required for a point s, belonging to root locus, to actually be selected as a desired closed-loop pole is computed according to the magnitude condition (5.6)**:

$$k = \frac{\prod_{i=1}^{n} l_i}{\prod_{j=1}^{m} l_j}.$$

10. The points where the root locus passes through the imaginary axis can be determined using Routh's criterion (see Sect. 4.3).
11. **If an additional open-loop pole located on the left half-plane is considered, "instability tends to increase" in the closed-loop system. This effect is stronger as the additional pole is placed closer to the origin.**
Consider Fig. 5.7, where s represents a point that belongs to the root locus and the open-loop transfer function is assumed to have only the shown two poles without zeros. According to the angle condition (5.7):

$$-(\theta_{p1} + \theta_{p2}) = -180^\circ.$$

The poles at p_1 and p_2 are retained in Fig. 5.8, but an additional pole is considered at p_3. The angle condition (5.7) now becomes:

$$-(\theta_{p1} + \theta_{p2} + \theta_{p3}) = -180^\circ.$$

This means that the addition $\theta_{p1} + \theta_{p2}$ must be smaller in Fig. 5.8 with respect to Fig. 5.7, which is accomplished if point s in Fig. 5.7 moves to the right, as in Fig. 5.8, i.e., if the root locus bends toward the right in Fig. 5.8. It is easy to see that this effect is stronger, i.e., the root locus is further pushed to the right half-plane, as θ_{p3} is larger, i.e., as p_3 approaches the origin. This proves that and integral controller tends to produce instability in the closed-loop system.
12. **If an additional open-loop zero located on the left half-plane is considered, "stability tends to increase" in the closed-loop system. This effect is stronger as the additional zero is placed closer to the origin.**
Consider again Fig. 5.7. According to the angle condition (5.7):

$$-(\theta_{p1} + \theta_{p2}) = -180^\circ.$$

The poles at p_1 and p_2 are retained in Fig. 5.9, but an additional zero at z_1 is considered. The angle condition (5.7) now becomes:

$$\theta_{z1} - (\theta_{p1} + \theta_{p2}) = -180^\circ.$$

This means that the addition $\theta_{p1} + \theta_{p2}$ must be larger in Fig. 5.9 than in Fig. 5.7, which is accomplished if point s in Fig. 5.7 moves to the left as in Fig. 5.9, i.e., if the root locus bends toward the left in Fig. 5.9. It is easy to see that this effect is stronger, i.e., the root locus is pulled to the left, as θ_{z1} is larger, i.e., as z_1 is closer to the origin. This proves that a derivative controller tends to improve the stability of a closed-loop system.

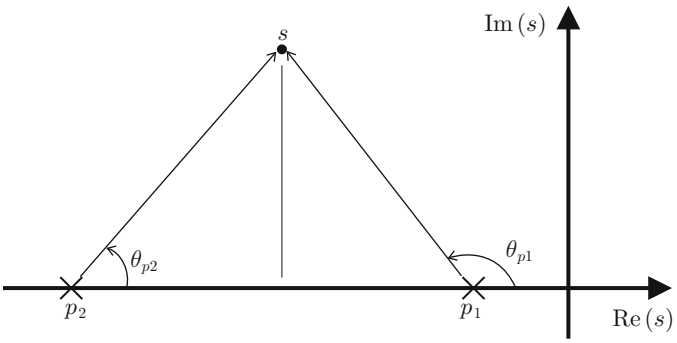

Fig. 5.7 A point belonging to the root locus for an open-loop system with two poles

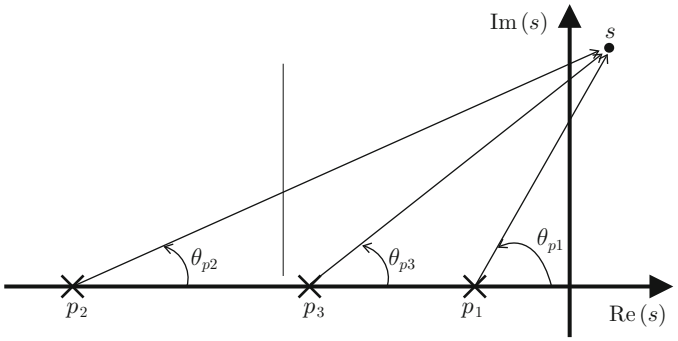

Fig. 5.8 The root locus is pushed toward the right when an additional open-loop pole is considered

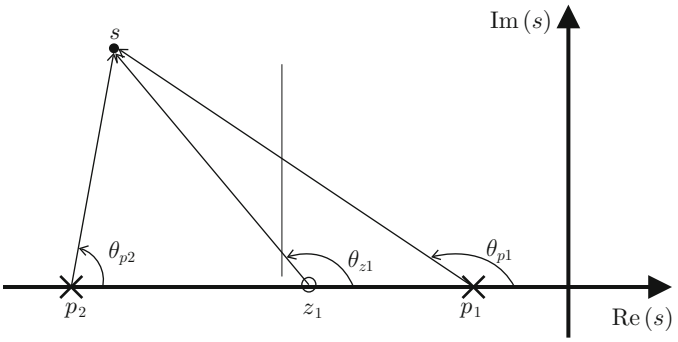

Fig. 5.9 The root locus is pulled toward the left when an additional open-loop zero is considered

5.2 Root Locus-Based Analysis and Design

5.2.1 Proportional Control of Position

According to Chap. 11, the permanent magnet brushed direct current (DC) motor model is given as:

$$\theta(s) = \frac{k}{s(s+a)} I^*(s), \tag{5.12}$$
$$a = \frac{b}{J} > 0, \quad k = \frac{nk_m}{J} > 0,$$

where $\theta(s)$ and $I^*(s)$ stand for the position and the electric current commanded respectively. Suppose that the following proportional position controller is employed:

$$I^*(s) = k_p(\theta_d(s) - \theta(s)),$$

where $\theta_d(s)$ is the desired position and k_p is a constant known as the proportional gain. The closed-loop system can be represented as in Fig. 5.10, where it is concluded that the open-loop transfer function is given as:

$$G(s)H(s) = \frac{k_p k}{s(s+a)}. \tag{5.13}$$

Notice that the system type is 1, i.e., the steady state error is zero when the desired position is a step. Hence, the only design problem that remains is to choose k_p such that the closed-loop poles are assigned to the desired locations. Use of the root locus method to solve this problem is shown in the following. The root locus method forces the gain k_p to take values from 0 to $+\infty$. First, $G(s)H(s)$ is rewritten as:

$$G(s)H(s) = \frac{k_p k}{l_1 l_2} \angle -(\theta_1 + \theta_2),$$

where the vectors $s - 0 = l_1 \angle \theta_1$ and $s - (-a) = l_2 \angle \theta_2$ have been defined (see Fig. 5.11). The fundamental conditions for drawing the root locus are the angle condition (5.7) and the magnitude condition (5.6) which are expressed respectively as:

$$-(\theta_1 + \theta_2) = \pm(2q+1)180^\circ, \quad q = 0, 1, 2, \ldots$$
$$\frac{k_p k}{l_1 l_2} = 1.$$

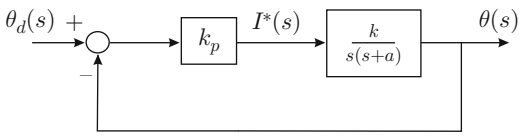

Fig. 5.10 Proportional position control system

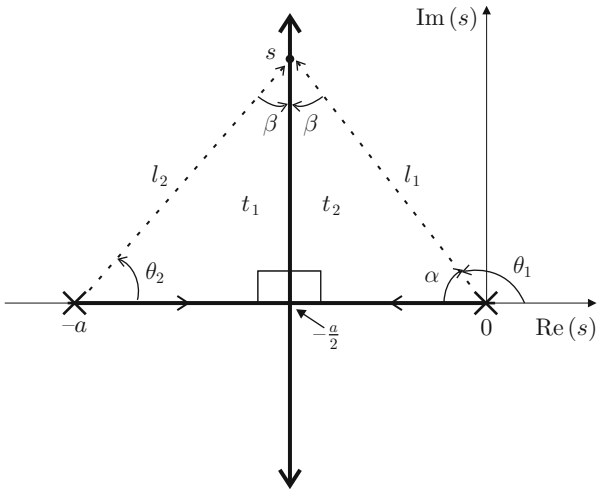

Fig. 5.11 Root locus for $G(s)H(s) = \frac{k_p k}{s(s+a)}$

Rule 5 indicates that, on the real axis, the root locus only exists between the points $s = 0$ and $s = -a$. Furthermore, according to rule 1, the root locus begins ($k_p = 0$) at $s = 0$ and $s = -a$. On the other hand, according to rules 2 and 3, the branches starting at $s = 0$ and $s = -a$ must approach some open-loop zero (no zero exists in this case) or some point at the infinity of the plane s as k_p tends to $+\infty$. Hence, the root locus has to move away from points $s = 0$ and $s = -a$, on the real axis, as k_p increases such that a breakaway point must exist somewhere between such points and then two branches appear to be moving away to infinity in plane s.

On the other hand, according to the angle condition, $-(\theta_1 + \theta_2) = -180^\circ = -(\alpha + \theta_1)$ in Fig. 5.11, it is concluded that $\alpha = \theta_2$, i.e., both triangles t_1 and t_2 must be identical for any closed-loop pole s. Hence, both branches referred above, which are shown in Fig. 5.11, must be parallel to the imaginary axis. This means that the breakaway point is located at the middle point between $s = 0$ and $s = -a$, i.e., at $(0 - a)/2 = -a/2$. This can also be verified using rules 3 and 4. Finally, according to rule 6, both branches are symmetrical with respect to the real axis.

The magnitude condition is employed when the exact value of k_p that renders a specific point of the root locus an actual closed-loop pole is required. Notice, for instance, that lengths l_1 and l_2 grow as k_p tends to $+\infty$ to satisfy the magnitude condition:

$$\frac{k_p k}{l_1 l_2} = 1, \tag{5.14}$$

which means that the closed-loop poles corresponding to large values of k_p tend to some point at infinity on the s plane. Hence, it is concluded: (i) Both closed-loop poles are real, negative, different, and approach the point $s = -a/2$ when $k_p > 0$ is small; this means that the closed-loop system becomes faster because the slowest pole moves away from the origin, (ii) According to the magnitude condition, when:

$$k_p = \frac{l_1 l_2}{k} = \frac{a^2}{4k}, \quad \text{with } l_1 = l_2 = \frac{a}{2},$$

both closed-loop poles are real, repeated, negative, and located at $s = -\frac{a}{2}$, i.e., the fastest response without oscillations is obtained, (iii) As $k_p > \frac{a^2}{4k}$ increases, both poles move away from the real axis (one pole moves upward and the other downward) on the vertical line passing through $s = -\frac{a}{2}$; this means that the closed-loop system becomes faster (because ω_n increases; see Sect. 3.3) and more oscillatory (because the angle $90° - \alpha$ decreases and damping, given as $\zeta = \sin(90° - \alpha)$, decreases; see Sect. 3.3).

The above discussion shows that it is not possible to achieve a closed-loop system response that is simultaneously fast and well damped. This is a direct consequence of the fact that closed-loop poles cannot be assigned at any arbitrary location of the s plane, as they can only be located on the thick straight line shown in Fig. 5.11. In the next example, it is shown that the introduction of an additional zero in the open-loop transfer function of the present example allows the closed loop poles to be assigned at any point on the s plane.

Example 5.1 The root locus diagram can also be plotted using MATLAB. Given a closed-loop system as that in Fig. 5.1, it suffices to use the command:

```
rlocus(GH)
```

where GH stands for the open-loop transfer function $G(s)H(s)$. Consider, for instance, the closed-loop system in Fig. 5.10 when $k = 2$ and $a = 8$. The root locus diagram in Fig. 5.12 is plotted using the following commands:

```
k=2;
a=8;
gh=tf(k,[1 a 0]);
rlocus(gh);
rlocfind(gh)
```

The root locus in Fig. 5.12 is represented by the continuous lines. Notice that, contrary to the previous discussion, in the above commands the proportional gain k_p is not considered. This is because k_p is automatically increased from 0 to $+\infty$ by MATLAB when executing the command "rlocus()". This must be taken into account when defining the open-loop transfer function to be used as an argument of this MATLAB command. In Fig. 5.12, each open-loop pole is represented by a symbol "×", i.e., at $s = 0$ and $s = -a = -8$. Compare Figs. 5.12 and 5.11 to verify similarities between them. For instance, the horizontal and vertical lines in

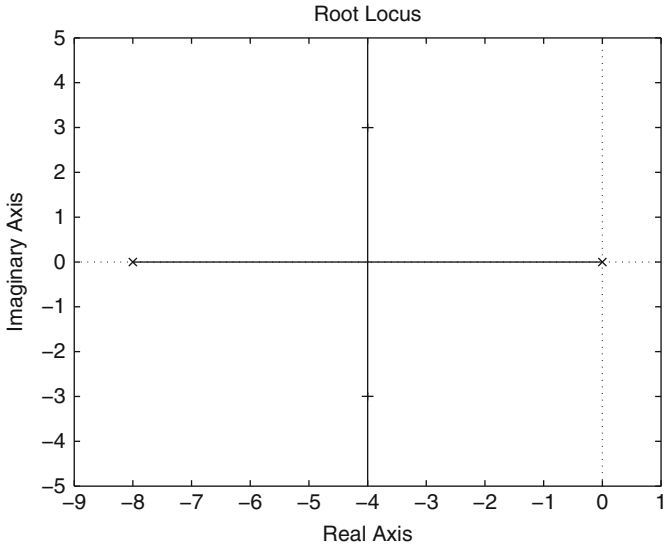

Fig. 5.12 Root locus for closed-loop system in Fig. 5.10

Fig. 5.12 intersect at $s = -4$, i.e., at $s = -a/2$, as predicted in Fig. 5.11. The root locus diagram is plotted by MATLAB when executing the command

```
rlocus(gh);
```

alone. However, the additional use of the command:

```
rlocfind(gh)
```

allows the user to select any desired point on the root locus. When selected, this point and all points on the root locus corresponding to the same gain k_p are marked with a symbol "+". For instance, in Fig. 5.12 the point $-4 + 3j$ was selected and, automatically, the point $-4 - 3j$ was also selected and marked with a "+" (only the horizontal line of this symbol is appreciable in Fig. 5.12 because of the particular geometry of this root locus). Also, MATLAB automatically sends the following text:

```
selected_point =
-3.9882 + 2.9969i
ans =
12.4907
```

This means that $k_p = 12.4907$ at $s = -4 \pm 3j$ and this can be verified using the magnitude condition in (5.14) as:

$$s - 0 = l_1 \angle \theta_1, \quad s - (-a) = l_2 \angle \theta_2,$$
$$l_1 = \sqrt{4^2 + 3^2} = 5, \quad l_2 = \sqrt{(8-4)^2 + 3^2} = 5,$$

$$k_p = \frac{l_1 l_2}{k} = \frac{25}{2} = 12.5.$$

When using the command "rlocus()", MATLAB automatically determines a maximal value of k_p to be considered to draw Fig. 5.12. However, the user can decide herself/himself the maximal value of k_p to be considered by using the command:

```
rlocus(gh,d);
```

where d is a vector containing all of the specific values of the gain k_p, which the user wants to be considered to plot the root locus.

Some closed-loop pole pairs are selected in Fig. 5.13. The time response of the closed-loop system Fig. 5.10 is presented in Fig. 5.14 when the corresponding closed-loop pole pairs are those indicated in Fig. 5.13. Recall that k_p increases as it passes from poles at "o" to poles at the square in Fig. 5.13. It is observed that the closed-loop system response becomes faster as k_p increases and overshoot is present once the closed-loop poles have imaginary parts that are different from zero. Moreover, overshoot is small if the imaginary parts are small. These observations corroborate the above root locus-based analysis.

The results in Figs. 5.13 and 5.14 were obtained by executing several times the following MATLAB code in an m-file:

```
k=2;
a=8;
kp=30; % 1 5 10 20 30
gh=tf(kp*k,[1 a 0]);
figure(1)
rlocus(gh);
hold on
rlocus(gh,34);
axis([-10 2 -9 9])
hold on
M=feedback(gh,1,-1);
v=pole(M);
figure(1)
plot(real(v(1)),imag(v(1)),'bs')
plot(real(v(2)),imag(v(2)),'bs')
figure(2)
step(M,'b:',5)
hold on
```

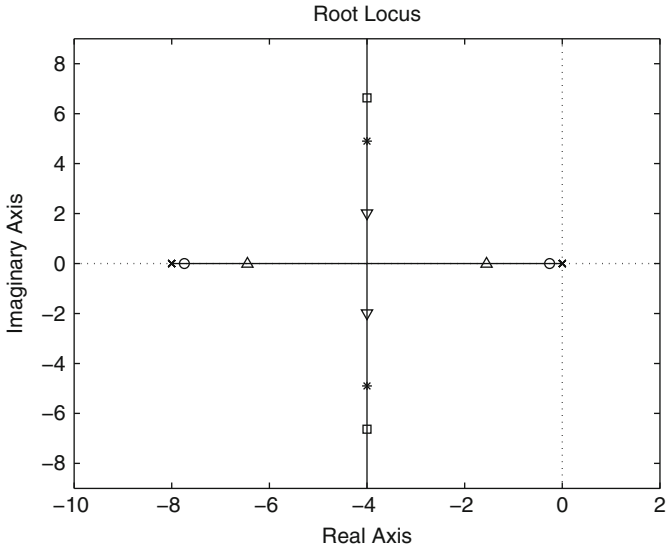

Fig. 5.13 Root locus in Fig. 5.12 when some closed-loop pole pairs are selected

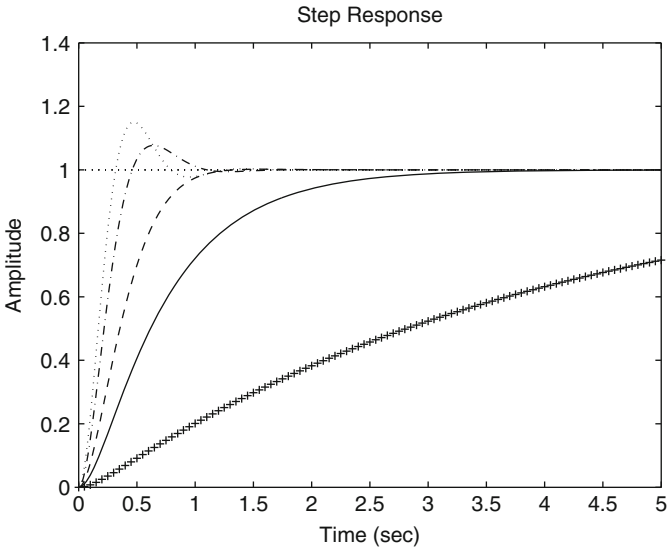

Fig. 5.14 Step response of the closed-loop system in Fig. 5.10, when the closed-loop poles are located as indicated in Fig. 5.13. The +line corresponds to poles at "o." The continuous line corresponds to poles at the triangle up. The dashed line corresponds to poles at the triangle down. The dash–dot line corresponds to poles at "*." The dotted line corresponds to poles at the square

5.2.2 *Proportional–Derivative Control of Position*

Consider again the motor model shown in (5.12), but now together with the following proportional–derivative (PD) controller:

$$i^* = k_p e + k_d \frac{de}{dt}, \quad e = \theta_d - \theta,$$

where k_p is the proportional gain and k_d is a constant known as the derivative gain. Use of the Laplace transform yields:

$$\begin{aligned} I^*(s) &= k_p E(s) + k_d s E(s), \\ &= (k_p + k_d s) E(s), \\ &= k_d \left(s + \frac{k_p}{k_d} \right) E(s). \end{aligned}$$

The corresponding closed-loop block diagram is shown in Fig. 5.15. The open-loop transfer function is given as:

$$G(s)H(s) = \frac{k_d k(s+c)}{s(s+a)}, \qquad c = \frac{k_p}{k_d} > 0. \tag{5.15}$$

Notice that, now, k_d is the gain that varies from 0 to $+\infty$ to plot the root locus. First, $G(s)H(s)$ is rewritten as:

$$G(s)H(s) = \frac{k_d k\, l_3}{l_1 l_2} \angle \theta_3 - (\theta_1 + \theta_2), \tag{5.16}$$

where the vectors $s - 0 = l_1 \angle \theta_1$, $s - (-a) = l_2 \angle \theta_2$, and $s - (-c) = l_3 \angle \theta_3$ have been defined. The angle and the magnitude conditions are expressed respectively as:

$$\begin{aligned} \theta_3 - (\theta_1 + \theta_2) &= \pm(2q+1)180^\circ, \quad q = 0, 1, 2, \ldots, \\ \frac{k_d k\, l_3}{l_1 l_2} &= 1. \end{aligned}$$

The root locus in this case can be obtained from the root locus obtained for the transfer function in (5.13) by simply taking into account that an additional zero at $s = -c$ has been included.

According to rule 12, the branches of the root locus in Fig. 5.11 will bend toward the left as a consequence of the additional zero. This can be verified using rule 3 to find that, now, the root locus only has one branch whose asymptote forms a $\pm 180^\circ$ with the positive real axis. As shown in Fig. 5.16, the root locus has two different possibilities depending on the exact location of the zero at $s = -c$. If it is placed at the left of the pole at $s = -a$ (as in Fig. 5.16a) then, according to rule 5, the root

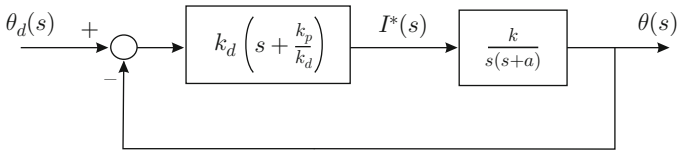

Fig. 5.15 Proportional–derivative (PD) control of position

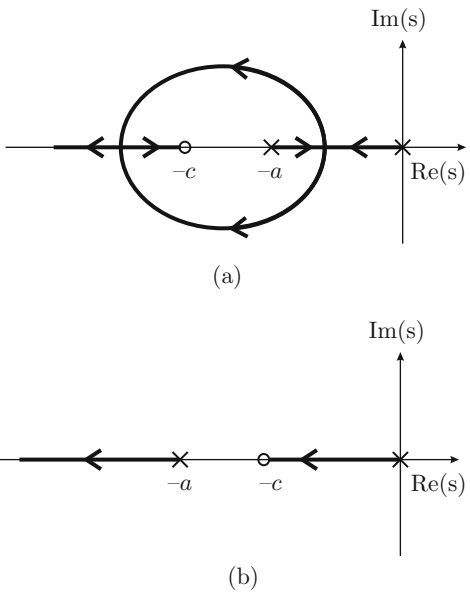

Fig. 5.16 Root locus for $G(s)H(s) = \frac{k_d k(s+c)}{s(s+a)}$. **(a)** $c > a$. **(b)** $c < a$

locus exists on two segments of the negative real axis: between the points $s = 0$ and $s = -a$, and to the left of zero at $s = -c$. Moreover, according to rules 2 and 3 one of the two root locus branches beginning ($k_d = 0$) at the open-loop poles located at $s = 0$ and $s = -a$ must tend toward the zero at $s = -c$ whereas the other branch must tend toward infinity in the s plane following the asymptote forming $\pm 180°$ with the positive real axis. Hence, a breakaway point must exist between points $s = 0$ and $s = -a$. Furthermore, as the root locus is symmetrical with respect to the real axis (rule 6), these branches must describe two semi circumferences toward the left of the breakaway point, which join again in a break-in point located on the negative real axis to the left of the zero at $s = -c$. After that, one branch approaches the zero at $s = -c$ and the other tends toward infinity along the negative real axis.

On the other hand, if the zero at $s = -c$ is placed between the open-loop poles at $s = 0$ and $s = -a$, then, according to rule 5, the root locus exists on two segments on the negative real axis located between points $s = -c$ and $s = 0$ and on the left of the pole at $s = -a$. Notice that, now, the branch beginning ($k_d = 0$) at $s = 0$ approaches the zero at $s = -c$, whereas the branch beginning ($k_d = 0$) at $s = -a$ tends toward infinity along the negative real axis. Also notice that this is possible without the necessity for any branch to exist outside the real axis, as is shown in Fig. 5.16b.

From the study of the resulting root locus, it is possible to realize that the closed-loop system is stable for any $k_p > 0$ and $k_d > 0$ because both possibilities for the root locus that have been presented in Fig. 5.16 show that the closed-loop poles are always located on the left half-plane s, i.e., the closed-loop poles have a negative real part. Finally, according to Sect. 3.8.3, there always exist gains k_p and k_d allowing any values to be chosen for both ω_n and ζ. This means that it is always possible to assign both closed-loop poles at any desired point on the left half-plane s.

Notice that the open-loop zero at $s = -c$ is also a zero of the closed-loop transfer function; hence, it also affects the closed-loop system transient response. This means that the transient response will not have the exact specifications computed using (3.71).

Example 5.2 The following MATLAB code is executed in an m-file to simulate the closed-loop system in Fig. 5.15:

```
clc
a=7;
k=70;
c=4; %7 4 10
Polo_des=-20;
l3=abs(Polo_des)-c;
l1=abs(Polo_des);
l2=abs(Polo_des)-a;
kd=l1*l2/(k*l3);
kp=c*kd;
Md=tf(20,[1 20]);
gm=tf(k,[1 a 0]);
PD=tf([kd kp],1);
M=feedback(gm*PD,1,-1);
v=pole(M)
%{
figure(1)
rlocus(gm*PD);
hold on
plot(real(v(1)),imag(v(1)),'k^');
plot(real(v(2)),imag(v(2)),'k^');
%}
figure(2)
step(Md*2,'r--',M*2,':',0.25)
hold on
```

It is assumed that $a = 7$ and $k = 70$. The desired response is that of a first-order system with time constant 0.05[s], i.e., with a real pole at $s = -20$. The idea is to propose different locations for the zero at $s = -c$ to observe when the desired response is accomplished. The derivative gain k_d is computed using the magnitude condition $\frac{k_d k\, l_3}{l_1 l_2} = 1$ where l_1, l_2, l_3 are the magnitude of the vectors defined in

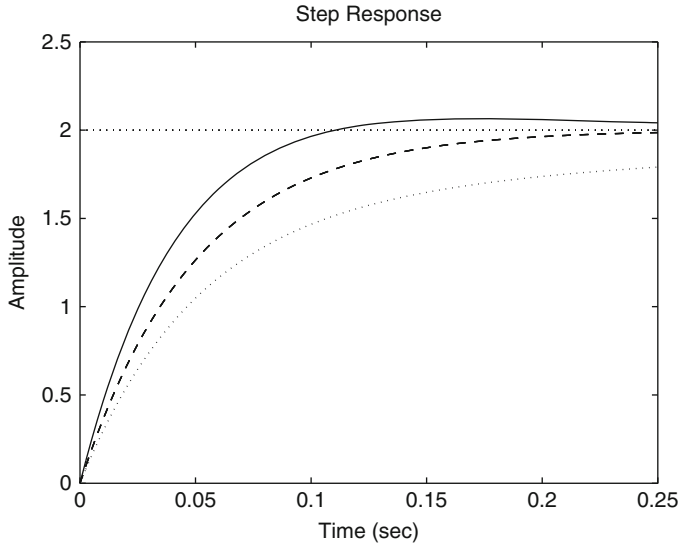

Fig. 5.17 Step response of the closed-loop system in Fig. 5.15, when a closed-loop first-order response with 0.05[s] time constant is desired. Dashed: desired response and closed-loop response when $c = a$. Dotted: closed-loop response when $c = 4$. Continuous: closed-loop response when $c = 10$

the paragraph after (5.16). Then $k_p = ck_d$ is computed. After that, it is possible to generate the closed-loop transfer function M and to simulate it together with the desired response. These results are shown in Fig. 5.17. Notice that the desired response is matched when $c = a$. The root locus diagram in this case is shown in Fig. 5.18 where the closed-loop poles are represented by a triangle up. One closed-loop pole is located at $s = -20$, as desired, and the other cancels with the zero at $s = -c$. This explains why the desired response is accomplished in this case.

When $c = 4$, the closed-loop poles are at $s = -20$, as desired, and $s = -3.25$. The latter pole is slow and does not cancel with zero at $s = -c = -4$; hence, its effects are important in the closed-loop transient response. This explains why, in this case, the response in Fig. 5.17 is slow. When $c = 10$, the closed-loop poles are located at $s = -20$ and $s = -13$, i.e., the pole at $s = -13$ cannot be cancelled by the zero at $s = -c$. This results in an overshoot, i.e., the desired response is not accomplished again. The reason for this overshoot is explained in Sect. 8.1.2, where it is stated that overshoot is unavoidable whenever all of the closed-loop poles are on the left of an open-loop zero despite all the closed-loop poles being real, i.e., as in the present case.

Example 5.3 The following MATLAB code is executed in an m-file to simulate the closed-loop system in Fig. 5.15:

```
clc
a=7;
```

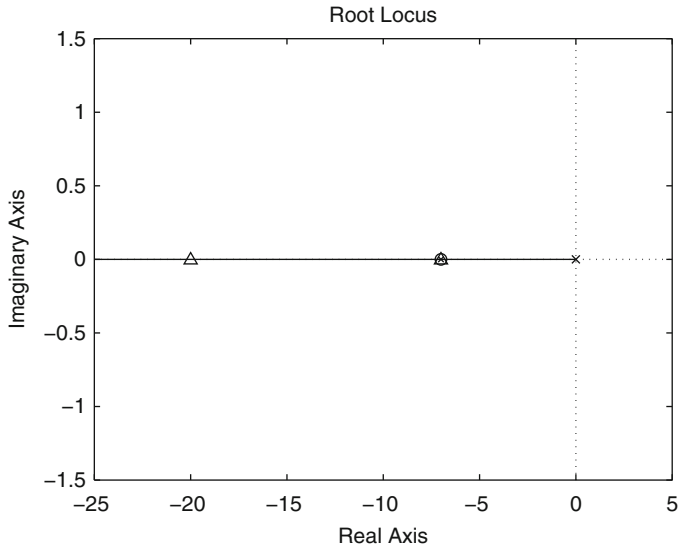

Fig. 5.18 Root locus corresponding to Fig. 5.15 when $c = a$

```
k=70;
tr=0.05;
Mp=14;%
z=sqrt( log(Mp/100)^2 /( log(Mp/100)^2 + pi^2 ) );
wn=1/(tr*sqrt(1-z^2))*(pi-atan(sqrt(1-z^2)/z));
s=-z*wn+wn*sqrt(1-z^2)*j
kd=(2*z*wn-a)/k;
kp=wn^2/k;
den1=conv([1 -s],[1 -real(s)+j*imag(s)]);
Md=tf(den1(3),den1);
gm=tf(k,[1 a 0]);
PD=tf([kd kp],1);
M=feedback(PD*gm,1,-1);
v=pole(M)
%%{
figure(1)
rlocus(gm*PD);
hold on
plot(real(v(1)),imag(v(1)),'k^');
plot(real(v(2)),imag(v(2)),'k^');
%}
figure(2)
step(Md*2,'r--',M*2,'-',0.25)
hold on
```

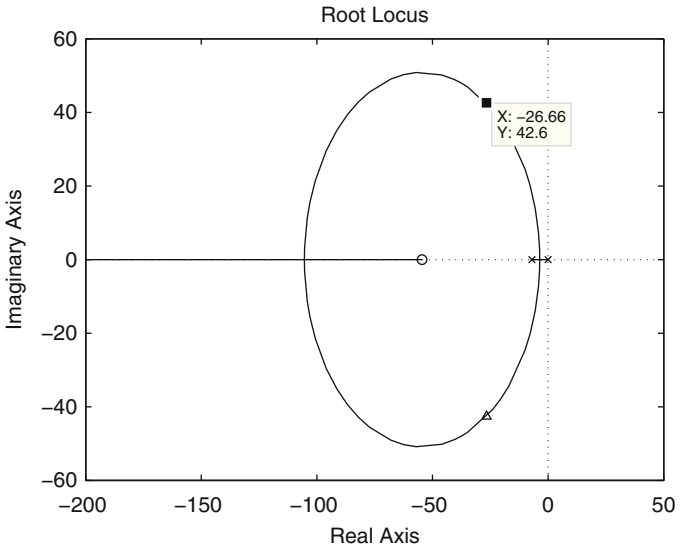

Fig. 5.19 Root locus diagram corresponding to Fig. 5.15 when $c > a$ and two closed-loop complex conjugate poles are specified (triangle up)

The desired specifications are a rise time of 0.05[s] and a 14% overshoot. This results in a pair of desired complex conjugate closed-loop poles located at $s = -26.66 \pm 42.59\,j$. The controller gains k_p and k_d were computed using:

$$k_d = \frac{2\zeta\omega_n - a}{k}, \quad k_p = \frac{\omega_n^2}{k},$$

(see Sect. 3.8.3). This allows the corresponding root locus diagram to be plotted in Fig. 5.19. Notice that this diagram is similar to that depicted in Fig. 5.16a because $c > a$ in this case. Although the desired closed-loop poles have been assigned, notice that the closed-loop zero at $s = -c$ cannot be cancelled; hence, it will modify the actual closed-loop response with respect to the desired one. As a matter of fact, in Fig. 5.20, the desired response, with a dashed line, and the actual closed-loop response, with a continuous line, are presented. We conclude that the effects of the zero at $s = -c$ are a shorter rise time and a larger overshoot.

5.2.3 *Position Control Using a Lead Compensator*

Consider again the DC motor model in (5.12) but, now, together with the following controller:

$$I^*(s) = \gamma \frac{s+d}{s+c}, \quad c > d > 0, \quad \gamma > 0,$$

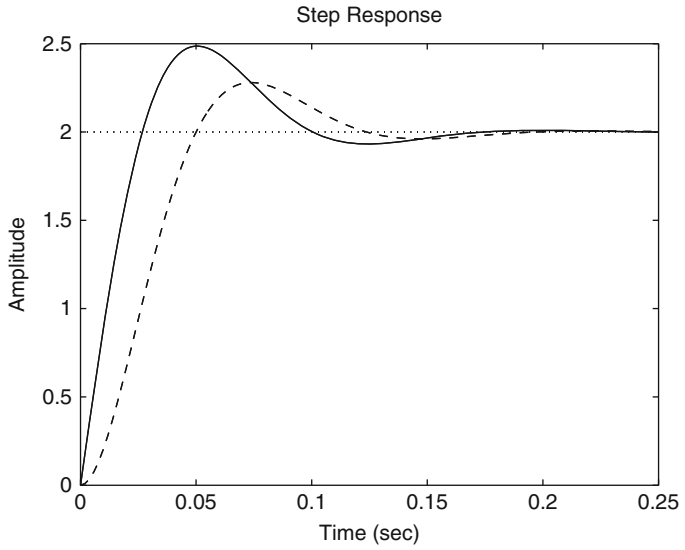

Fig. 5.20 Step response of the closed-loop system in Fig. 5.15, when $c > a$ and two closed-loop complex conjugate poles are specified. Dashed: desired response. Continuous: closed-loop response

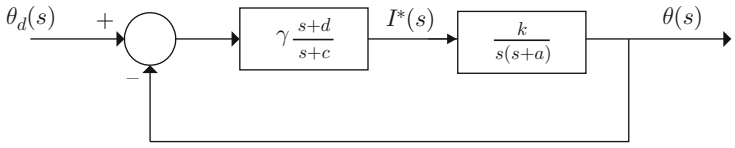

Fig. 5.21 Position control using a lead compensator

which is known as a lead compensator if $c > d$. This condition is introduced when it is desired to increase the damping in the system, i.e., when the closed-loop poles must be shifted to the left (see rules 11 and 12). The corresponding closed-loop block diagram is shown in Fig. 5.21. The open-loop transfer function is given as:

$$G(s)H(s) = \gamma \frac{k(s+d)}{s(s+a)(s+c)}. \tag{5.17}$$

If d is chosen as:

$$d = a, \tag{5.18}$$

then the close-loop transfer function is:

$$\frac{\theta(s)}{\theta_d(s)} = \frac{\gamma k}{s^2 + cs + \gamma k} = \frac{\omega_n^2}{s^2 + 2\zeta\omega_n s + \omega_n^2},$$

which means that:

$$c = 2\zeta\omega_n, \quad \gamma = \frac{\omega_n^2}{k}. \tag{5.19}$$

Hence, if the expressions in (3.71) are used to compute ζ and ω_n such that the desired rise time and overshoot are obtained, then (5.18) and (5.19) represent a simple tuning rule. Moreover, the formulas in (3.71) for overshoot and rise time are exact in this case; thus, the drawback that a PD controller has in this respect is eliminated. The transient response in this case is rather similar to that obtained with the controller in Sect. 3.8.2, i.e., proportional position control plus velocity feedback.

5.2.4 *Proportional–Integral Control of Velocity*

Although proportional–integral (PI) velocity control has been studied in Sect. 3.8.4, in this part, some ideas are presented that are clearer when employing block diagrams and the root locus. According to Chap. 10, when the velocity $\omega(s)$ is the output, the permanent magnet brushed DC motor model is:

$$\omega(s) = \frac{1}{s+a}[kI^*(s) - \frac{1}{J}T_p(s)],$$
$$a = \frac{b}{J} > 0, \quad k = \frac{nk_m}{J} > 0,$$

where the commanded electric current $I^*(s)$ is the input and $T_p(s)$ is an external torque disturbance. A PI velocity controller is given as:

$$i^* = k_p e + k_i \int_0^t e(r)dr, \quad e = \omega_d - \omega,$$

where ω_d is the desired velocity, k_p is the proportional gain and the constant k_i is known as the integral gain. Using the Laplace transform:

$$\begin{aligned} I^*(s) &= k_p E(s) + k_i \frac{E(s)}{s}, \\ &= \left(k_p + \frac{k_i}{s}\right) E(s), \\ &= \left(\frac{k_p s + k_i}{s}\right) E(s), \\ &= k_p \left(\frac{s + \frac{k_i}{k_p}}{s}\right) E(s). \end{aligned}$$

Hence, the closed-loop block diagram is depicted in Fig. 5.22a. As this control system has two inputs, the superposition principle can be employed (see Sect. 3.7) to write:

$$\omega(s) = G_1(s)\omega_d(s) + G_2(s)T_p(s),$$

where $G_1(s)$ is the transfer function obtained when using $\omega_d(s)$ as the input and $\omega(s)$ as the output and assuming $T_p(s) = 0$, i.e., using the block diagram in Fig. 5.22b, whereas $G_2(s)$ is the transfer function when $T_p(s)$ is the input and $\omega(s)$ is the output, assuming that $\omega_d(s) = 0$, i.e., when using the block diagram in Fig. 5.22c. It is important to say that, in the case when $T_p(s)$ is the input, $\omega(s)$ represents the velocity deviation produced by disturbance $T_p(s)$.

Now, the problem of choosing the PI controller gains such that the transient response of the closed-loop system satisfies the desired specifications is studied. It is observed in Fig. 5.22b, that the open-loop transfer function is:

$$G(s)H(s) = \frac{k_p k(s+c)}{s(s+a)}, \quad c = \frac{k_i}{k_p}, \tag{5.20}$$

Notice that the system type is 1, which ensures that $\omega(t) = \omega_d$ in a steady state if ω_d is a constant. This is one reason for using a PI controller in this example. Hence, the only problem that remains is to choose the controller gains k_p and k_i, such that the transient response satisfies the desired specifications. To this aim, notice that the open-loop transfer function shown in (5.20) is identical to the transfer function shown in (5.15), which corresponds to the PD control of position as only k_d has to be replaced by k_p. Thus, the root locus diagram corresponding to the PI velocity control is identical to both cases shown in Fig. 5.16 and the same conclusions are obtained:

i) There always exist some gains k_p and k_i allowing both closed-loop poles to be placed at any point on the left half-plane; hence, it is possible to tune the PI controller using a trial and error procedure (see Sect. 3.8.4).

ii) The open-loop zero located at $s = -c$ is also a zero of the closed-loop transfer function $G_1(s)$, i.e., it also affects the closed-loop transient response. This means that the transient response does not have the specifications designed using (3.71) to choose the closed-loop poles. This poses the following two possibilities.

1. The problem pointed out at *ii*) can be eliminated if it is chosen:

$$c = a = \frac{k_i}{k_p}, \tag{5.21}$$

because, in such a case and according to Fig. 5.22b and (5.1), the closed-loop transfer function is:

$$\frac{\omega(s)}{\omega_d(s)} = \frac{k_p k}{s + k_p k}.$$

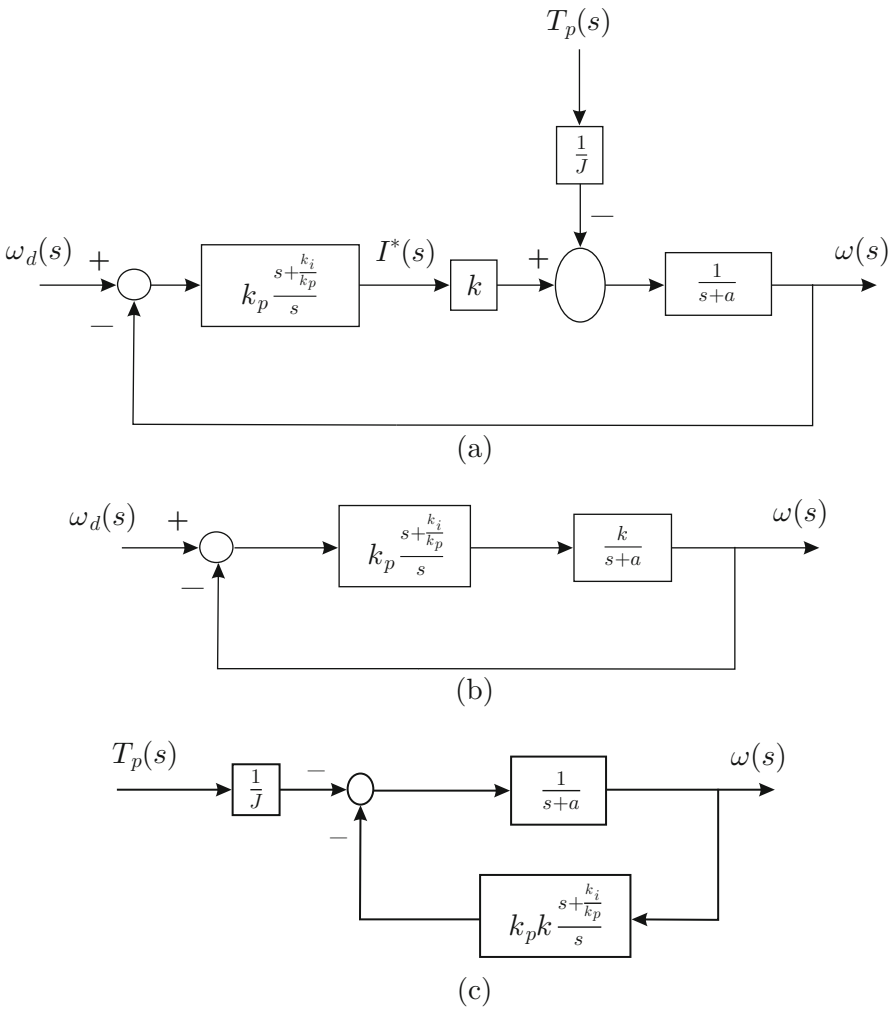

Fig. 5.22 Proportional–integral control of velocity . (**a**) The complete control system. (**b**) $T_p(s) = 0$. (**c**) $\omega_d(s) = 0$

This means that the closed-loop response is as that of a first-order system with a unit steady state gain and a time constant given as $\frac{1}{k_pk}$. Then, if a time constant τ is specified:

$$k_pk = \frac{1}{\tau}. \tag{5.22}$$

The conditions in (5.22) and (5.21) represent a simple tuning rule. Finally, the root locus diagram corresponding to this case ($c = a$, $G(s)H(s) = \frac{k_pk}{s}$) is shown

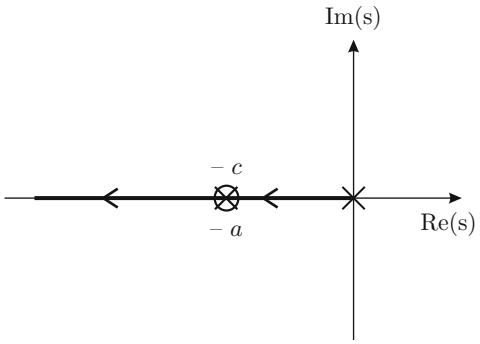

Fig. 5.23 Root locus for $c = a$, $G(s)H(s) = \frac{k_p k}{s}$

in Fig. 5.23. This can be easily verified using rules 3 and 5. As there is only one open-loop pole, there is only one closed-loop pole, which must be real and tends toward one zero at infinity (on an asymptote forming $-180°$ with the positive real axis) because there is no open-loop zero. Furthermore, the magnitude condition:

$$\frac{k_p k}{l_1} = 1,$$

where l_1 is the distance from the desired closed-loop pole to the origin, establishes that the desired closed-loop pole located at $s = -\frac{1}{\tau}$ is reached when:

$$k_p k = l_1, \quad l_1 = \frac{1}{\tau} \Rightarrow k_p k = \frac{1}{\tau},$$

which corroborates (5.22). However, this tuning rule has a problem when considering the closed-loop response when an external disturbance $T_p(s)$ appears. Consider the block diagram in Fig. 5.22c. If $c = a$ is chosen, then the closed-loop transfer function is:

$$\frac{\omega(s)}{T_p(s)} = \frac{-\frac{k}{J}s}{(s + k_p k)(s + a)}. \tag{5.23}$$

Using the final value theorem, the following is found:

$$\begin{aligned} \lim_{t\to\infty} \omega(t) &= \lim_{s\to 0} s\omega(s), \\ &= \lim_{s\to 0} s \frac{-\frac{k}{J}s}{(s + k_p k)(s + a)} \frac{t_d}{s} = 0, \end{aligned}$$

i.e., that the velocity deviation produced by the external torque disturbance with a constant value t_d vanishes in a steady state. This is the reason why a PI velocity controller is chosen. However, there is a problem. The poles of the transfer

function in (5.23) determine how fast this velocity deviation vanishes. These poles are located at $s = -k_p k$ and $s = -a$. Although one of these poles can be rendered as fast as desired just by choosing a suitable k_p, the other pole, at $s = -a$, cannot be modified and depends on the parameters of the DC motor. This has as a consequence that the velocity deviation due to the disturbance may approach zero very slowly, which is a serious drawback.

2. Trying to solve the above problem, we might abandon the tuning rule in (5.22) and (5.21). As we now have $c \neq a$, the closed-loop transfer function corresponding to the block diagram in Fig. 5.22c is:

$$\frac{\omega(s)}{T_p(s)} = \frac{-\frac{k}{J}s}{s^2 + (a + k_p k)s + k_p k c}. \tag{5.24}$$

Using the final value theorem, it can be easily verified that, in the case of a constant disturbance $T_p(s) = \frac{t_d}{s}$, the steady-state deviation is zero again: $\lim_{t\to\infty} \omega(t) = 0$, because the transfer function in (5.24) has a zero at $s = 0$. On the other hand, poles of the transfer function in (5.24), which determine how fast the velocity deviation vanishes, are identical to the poles of the transfer function $\frac{\omega(s)}{\omega_d(s)} = G_1(s)$; hence, they can be assigned using the root locus method from (5.20). As has been explained, the corresponding root locus is identical to both cases shown in Fig. 5.16 replacing k_d by k_p. It is important to stress that the transfer function in (5.24) has no zero at $s = -c$ shown in the root locus diagram in Fig. 5.16. This means that none of the closed-loop poles obtained using the root locus method can cancelled with the zero at $s = -c$ and the slowest pole will have the most significant effect on the time required for the velocity deviation due to the disturbance to vanish. With these ideas in mind, the following is concluded.

- To render small the effect of the zero at $s = -c$ on the transient response to a given velocity reference, one closed-loop pole must be placed close to the zero at $s = -c$. The other closed-loop pole (the fastest one) moves away to the left and tends toward infinity as the slow pole approaches to $s = -c$.
- This means that the fast pole determines the transient response, i.e., the time constant, to a given velocity reference. Then, if it is desired to fix some finite value for the time constant (such that the fast pole is placed at a finite point on the negative real axis), the slow pole is always relatively far from zero at $s = -c$. This means that the transient response is always affected by both poles and the zero at $s = -c$. Hence, if $c \neq a$, a tuning rule cannot be determined such that transient response to a given velocity reference satisfies the desired specifications. Notice that this is also true if the response to a reference is specified by two complex conjugate poles, as the zero at $s = -c$ cannot be cancelled; hence, it has the effect of modifying the transient response with respect to that specified by the two complex conjugate poles.

- It is more convenient to select $c > a$ because the slowest closed-loop pole (that approaching $s = -c$) is shifted further to the left (it is faster) compared with the case when $c < a$ is chosen.
- This also implies that, if it is desired that the velocity deviation due to a disturbance vanishes faster, we must choose $c \neq a$ with $c > 0$ larger. According to $c = k_i/k_p$, this means that a larger integral gain is obtained.

Thus, although it is possible to render shorter the time it takes to the velocity deviation due to disturbance to vanish, it is concluded that the controller gains k_p y k_i cannot be exactly computed to ensure that, simultaneously, the desired transient response specifications to a given velocity reference are accomplished and that the disturbance effects vanish as fast as desired. This statement is verified experimentally in Chap. 10 and, because of this, in that chapter a modified PI velocity controller is introduced, solving this situation.

Anticipating its experimental use in Chap. 10, a tuning rule is proposed next for the case when $c \neq a$. According to (5.20), the magnitude condition is:

$$\frac{k_p k l_1}{l_3 l_2} = 1,$$

where $s - (0) = l_2 \angle \theta_2$, $s - (-a) = l_3 \angle \theta_3$, and $s - (-c) = l_1 \angle \theta_1$. According to this tuning criterion, propose the slowest pole to be located at some known $s = -p_1$, to fix an upper limit on the time required to render negligible the disturbance effect. On the other hand, according to the items listed above, c is proposed to be close to p_1 such that $p_1 > c$. Then, using the magnitude condition above, the following tuning rule is obtained:

$$\frac{k_i}{k_p} = c, \quad c < p_1, \quad k_p = \frac{l_2 l_3}{l_1 k}, \tag{5.25}$$
$$l_1 = abs(-p_1 + c), \quad l_2 = abs(-p_1), \quad l_3 = abs(-p_1 + a).$$

According to the discussion above, the response to the reference of velocity is much faster than predicted by the pole at $s = -p_1$. For comparison purposes this is very important as some velocity controllers are designed in Chap. 10 accomplishing simultaneously transient responses to a velocity reference and to an external disturbance that are determined by a pole at $s = -p_1$. On the contrary, with the PI velocity controller studied in this section, if it is desired that the response to an external disturbance is faster (with a pole at $s = -p_1$), the response to a desired reference of velocity must be much faster.

Example 5.4 The MATLAB/Simulink diagram corresponding to Fig. 5.22a is shown in Fig. 5.24. It is assumed that $k = 70$ and $a = 7$. The desired velocity ω_d is a step command with 2 as the magnitude. The disturbance T_p is a step applied at $t = 2$[s] with a magnitude 0.4×70. The PI controller block has k_p and k_i as proportional and integral gains.

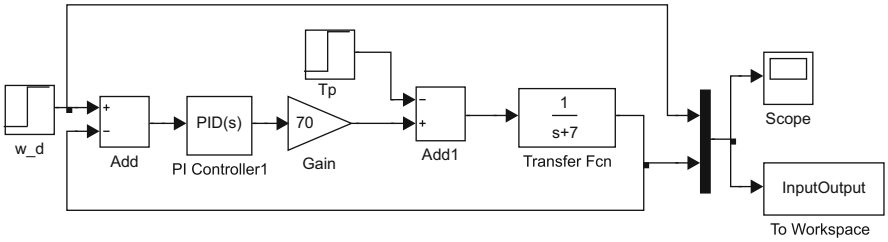

Fig. 5.24 MATLAB/Simulink diagram corresponding to the closed-loop system in Fig. 5.22a

The simulation in Fig. 5.24, was performed with the help of the following MATLAB code in an m-file:

```
a=7;
k=70;
Polo_des=-20;
c=15; %1 5 7 10 15
l1=abs(Polo_des)-c;
l2=abs(Polo_des);
l3=abs(Polo_des)-a;
kp=l2*l3/(k*l1);
ki=c*kp;
PI=tf(kp*[1 c],[1 0]);
gm=tf(k,[1 a]);
M=feedback(PI*gm,1,-1);
figure(1)
gd=tf(20,[1 20]);
step(M*2,'b:',gd*2,'r--',0.2)
hold on
%%{
nn=length(InputOutput(:,2));
n=nn-1;
Ts=10/n;
t=0:Ts:10;
figure(2)
plot(t,InputOutput(:,2),'k:');
axis([-0.5 10 0 2.5])
xlabel('t [s]')
ylabel('w [rad/s]')
hold on
%}
```

In this code, the desired closed-loop response is specified to be as that of a first-order system with a time constant $\tau = \frac{1}{20} = 0.05$[s] when a desired step velocity is commanded. This desired response is shown in Fig. 5.25 with a dashed line. The

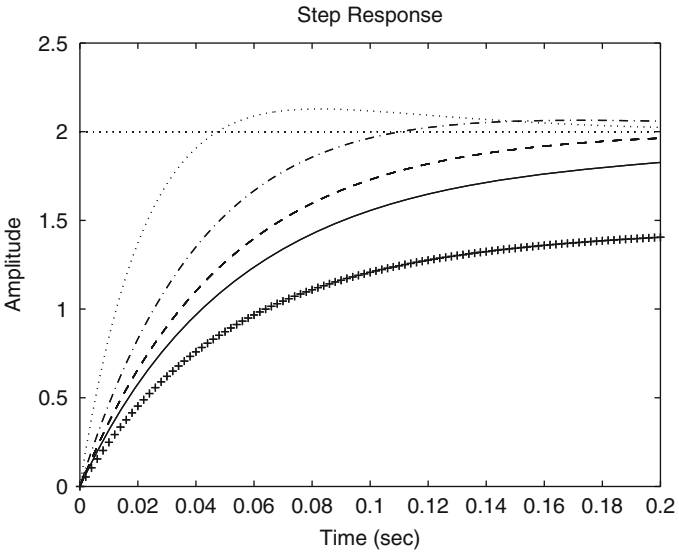

Fig. 5.25 Response to a step command in desired velocity $\omega_d(s)$

design criterion is to find k_p and k_i such that the desired closed-loop pole is assigned at $s = -20$, provided that a ratio $\frac{k_i}{k_p}$ is given. This allows to the system response to be analyzed when the integral gain is enlarged and one closed-loop pole is at the desired location.

First, the location of zero at $-\frac{k_i}{k_p} = -c$ is fixed by defining the constant c. The proportional gain k_p is computed using the magnitude condition $\frac{k_p k l_1}{l_3 l_2} = 1$, where l_1, l_2, l_3, are the magnitudes of vectors defined in the paragraph before (5.25), and $k_i = ck_p$ is also computed. Then, the closed-loop transfer function is obtained and the closed-loop system response as well as the desired response can be simulated using the command "step()". These signals are shown in Fig. 5.25. At this point, the simulation diagram in Fig. 5.24 is run and, with the help of the remaining code lines above, the corresponding results are shown in Fig. 5.26.

In Figs. 5.25 and 5.26 the following data are presented. (i) The line marked with "+" corresponds to $c = 1$, (ii) Continuous line: $c = 5$, (iii) Dashed line: $c = 7$, (iv) Dash–dot line: $c = 10$, and (v) Dotted line: $c = 15$. Notice that the disturbance effect is rejected very slowly when $c = 1$. In this case, the closed-loop poles are at $s = -20$ and $s = -0.6842$, which can be verified using the MATLAB command "pole(M)". Recall that the transfer function in (5.24) has no zero to cancel the pole at $s = -0.6842$.[2] This explains the slow rejection of the disturbance effects in this case. Also notice that the response to the velocity reference is also slow. This is because the effect of the pole at $s = -0.6842$ is not suitably cancelled by the zero at $s = -c = -1$.

[2]If it is assumed that this pole and zero at $s = 0$ cancel each other out, then a nonzero steady-state deviation would exist and the problem would be worse.

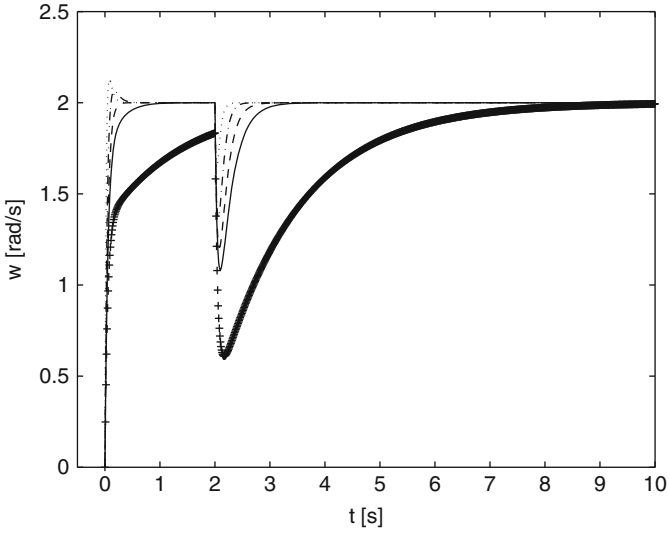

Fig. 5.26 Response to a step disturbance $T_p(s)$

Notice that the disturbance rejection and the response to the reference improve as c increases. Moreover, the system response exactly matches the desired response when $c = 7 = a$. However, the disturbance effects are still important in this case. When $c > 7 = a$, the disturbance rejection further improves, but the response to the reference exhibits overshoot, i.e., it is no longer a first-order response. According to Sect. 8.1.2, this behavior appears, and it is unavoidable, when the closed-loop poles are on the left of an open-loop zero. In this respect, notice that the closed-loop poles are at $s = -20$ and $s = -13$ when $c = 10$ and at $s = -20$ and $s = -39$ when $c = 15$.

The simulation results in this example corroborate the system behavior predicted in the above discussion, i.e., the classical PI control has limitations when it is required to satisfy simultaneously a specified response to a reference and a specified performance for disturbance rejection.

5.2.5 Proportional–Integral–Derivative Control of Position

Consider again the DC motor model but, now, assuming the presence of an external disturbance:

$$\theta(s) = \frac{1}{s(s+a)}[kI^*(s) - \frac{1}{J}T_p(s)],$$

together with the following proportional–integral–derivative controller:

$$i^* = k_p e + k_d \frac{de}{dt} + k_i \int_0^t e(r)dr, \quad e = \theta_d - \theta,$$

where θ_d is the desired position and the constants k_p, k_d and k_i are known as the proportional, derivative, and integral gains respectively. Use of the Laplace transform, yields:

$$\begin{aligned} I^*(s) &= k_p E(s) + k_d s E(s) + k_i \frac{E(s)}{s}, \\ &= \left(k_p + k_d s + \frac{k_i}{s} \right) E(s), \\ &= k_d \frac{s^2 + \frac{k_p}{k_d} s + \frac{k_i}{k_d}}{s} E(s), \end{aligned}$$

and the corresponding block diagram is shown in Fig. 5.27a. As this is a system with two inputs, the superposition principle (see Sect. 3.7) can be used to write:

$$\theta(s) = G_1(s)\theta_d(s) + G_2(s)T_p(s),$$

where $G_1(s)$ is the closed-loop transfer function when $\theta_d(s)$ is the input and $\theta(s)$ is the output with $T_p(s) = 0$, i.e., when the block diagram in Fig. 5.27b is used to find:

$$\frac{\theta(s)}{\theta_d(s)} = G_1(s) = \frac{k_d k \left(s^2 + \frac{k_p}{k_d} s + \frac{k_i}{k_d} \right)}{s^3 + (a + k_d k)s^2 + k_p k s + k_i k}, \quad T_p(s) = 0. \tag{5.26}$$

On the other hand, $G_2(s)$ is the closed-loop transfer function when $T_p(s)$ is the input and $\theta(s)$ is the output with $\theta_d(s) = 0$, i.e., when the block diagram in Fig. 5.27c is employed to write:

$$\frac{\theta(s)}{T_p(s)} = G_2(s) = \frac{-\frac{k}{J} s}{s^3 + (a + k_d k)s^2 + k_p k s + k_i k}, \quad \theta_d(s) = 0. \tag{5.27}$$

It is stressed that when $T_p(s)$ is the input, then $\theta(s)$ stands for the position deviation (with respect to $\theta_d(s)$) produced by the external disturbance. Using the final value theorem, it is found that:

$$\begin{aligned} \lim_{t \to \infty} \theta(t) &= \lim_{s \to 0} s\theta(s), \\ &= \lim_{s \to 0} s \frac{-\frac{k}{J} s}{s^3 + (a + k_d k)s^2 + k_p k s + k_i k} \frac{t_d}{s} = 0, \end{aligned}$$

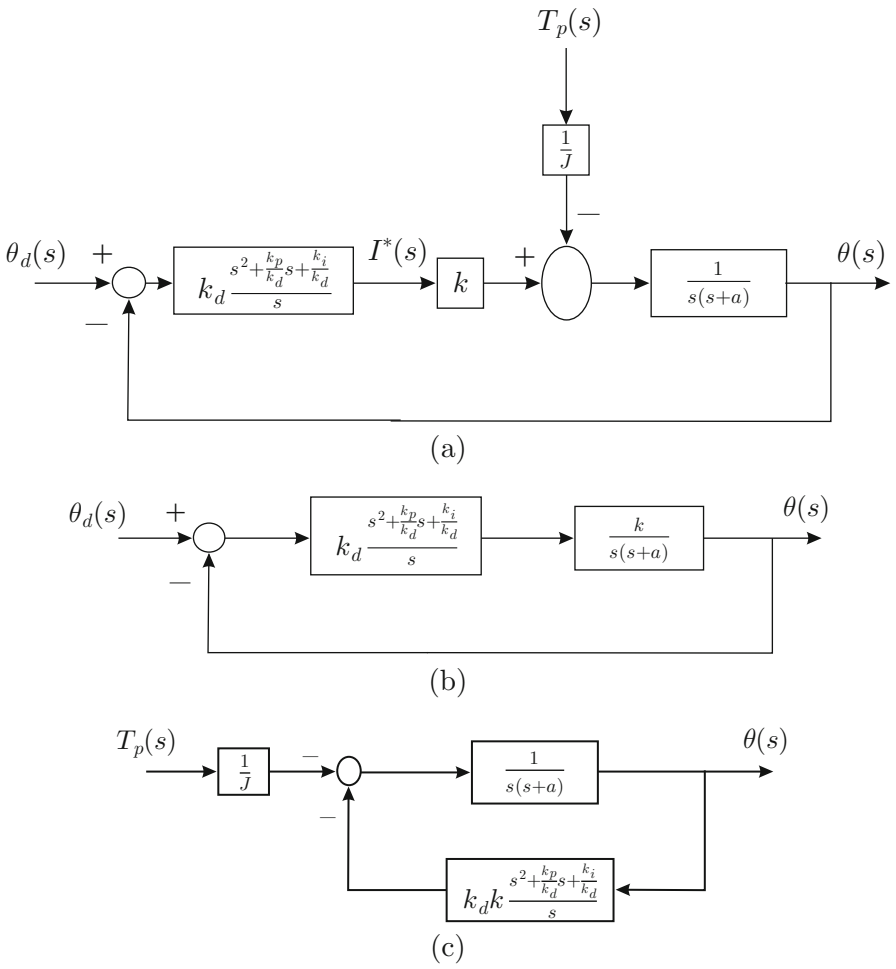

Fig. 5.27 Proportional–integral–derivative (PID) position control . (**a**) The complete control system. (**b**) $T_p(s) = 0$. (**c**) $\theta_d(s) = 0$

the deviation of position produced by the constant external torque disturbance $T_p(s) = \frac{t_d}{s}$ is zero in a steady state. Using the final value theorem again, it is not difficult to verify that, using (5.26), the final value of position θ is equal to the desired value θ_d when this is a constant. These are the main reasons for using a PID position controller.

The problem of choosing the controller gains for the PID controller such that the closed-loop response has the desired transient response specifications when a position reference θ_d is applied is studied in the following. To this aim, the three poles of the transfer function in (5.26) must be assigned at the desired locations on the left half-plane. This is accomplished by equating the characteristic polynomial

of the transfer function in (5.26) to a polynomial with roots at the desired points $s = p_1, s = p_2, s = p_3$:

$$s^3 + (a + k_d k)s^2 + k_p k s + k_i k = (s - p_1)(s - p_2)(s - p_3).$$

It is clear that any values can be assigned to the coefficients of the characteristic polynomial by using suitable combinations of the controller gains k_p, k_d and k_i. This means that the three poles of the closed-loop system can be assigned at any desired location of the left half-plane. Any set of three poles satisfying this requirement can be written as:

$$p_1 = \sigma_1 + j\omega_1, \quad p_2 = \sigma_2 - j\omega_1, \quad p_3 < 0, \quad \sigma_1 < 0, \quad \sigma_2 < 0, \quad \omega_1 \geq 0.$$

Notice that $\sigma_1 = \sigma_2$ if $\omega_1 > 0$, i.e., when a pair of complex conjugate poles exists, but $\sigma_1 \neq \sigma_2$ is possible when $\omega_1 = 0$. Hence:

$$s^3 + (a + k_d k)s^2 + k_p k s + k_i k = (s - p_1)(s - p_2)(s - p_3),$$
$$s^3 - (p_1 + p_2 + p_3)s^2 + (p_1 p_2 + p_3 p_1 + p_3 p_2)s - p_1 p_2 p_3.$$

Equating the coefficients and using the above data, the following tuning rule is obtained:

$$k_d = \frac{-(\sigma_1 + \sigma_2 + p_3) - a}{k} > 0, \tag{5.28}$$
$$k_p = \frac{\sigma_1\sigma_2 + \omega_1^2 + p_3\sigma_1 + \sigma_2 p_3}{k} > 0,$$
$$k_i = \frac{-p_3(\sigma_1\sigma_2 + \omega_1^2)}{k} > 0.$$

It is stressed that the three controller gains are positive. As a rule of thumb, if $-p_3 > 6|\sigma_1|$ then the real and imaginary parts of the poles at p_1 and p_2 can be computed using (3.71) such that the desired rise time t_r and overshoot $M_p(\%)$ are obtained. However, the system response presents some important differences with respect to these values because of the pair of zeros contained in the transfer function in (5.26). Although this is an important drawback of the tuning rule in (5.28), these values can be used as rough approximations of the required gains for the controller to perform fine adjustments afterward, by trial and error, until the desired transient response specifications are accomplished. To this aim, as the closed-loop system is third order, it is important to recall the stability rule obtained in Example 4.12 of Sect. 4.3. The possibility of adjusting the gains of a PID controller by trial and error (see Sect. 5.3) is one of the main reasons for the success of PID control in industry.

With the aim of finding a tuning rule allowing to exactly compute the gains of a PID controller, the root locus method is employed in the following. From the block diagram in Fig. 5.27b, it is concluded that the open-loop transfer function is given as:

$$G(s)H(s) = \frac{k_d k(s+\alpha)(s+\beta)}{s^2(s+a)}, \quad (s+\alpha)(s+\beta) = s^2 + \frac{k_p}{k_d}s + \frac{k_i}{k_d}, \tag{5.29}$$

for some constants α and β different from zero whose values are proposed as part of the design process. Then, from these values both k_p and k_i are computed. Notice that k_d is the gain that the method varies from 0 to $+\infty$ to plot the root locus diagram. It is clear that the system type is 2 (the motor is naturally provided with an integrator and another integrator is introduced by PID controller) and, hence, the steady-state error is zero if the reference of the position is constant.

Three possibilities for the corresponding root locus diagram are presented in Fig. 5.28. They depend on the values proposed for α and β. The reader is encouraged to use the rules introduced in Sect. 5.1.1 to corroborate these results. According to Fig. 5.28a, it is possible to design the control system such that two closed-loop poles are close to the zeros located at $s = -\alpha$ and $s = -\beta$. This would allow the closed-loop system to respond as a first-order system with one real and negative pole. One closed-loop pole may also be chosen to be close to the zero at $s = -\alpha$ such that the closed-loop system responds as a second-order system with complex conjugate poles and one real zero. Although the presence of this zero modifies the transient response, this is one way of specifying the transient response in terms of rise time and overshoot. This is the design criterion used in the following.

In cases like this one, the traditional root locus-based design procedures suggest performing the following three steps:

- Design a PD controller with transfer function:

  $$k_d(s+\beta),$$

  such that some desired rise time and overshoot are accomplished.
- Given the open-loop transfer function designed in the previous step, introduce the following factor:

  $$\frac{s+\alpha}{s},$$

  with α some positive value close to zero.
- Compute the PID controller gains using (5.29), i.e.,

  $$k_p = (\alpha+\beta)k_d, \quad k_i = \alpha\beta k_d. \tag{5.30}$$

Now, the PD controller $k_d(s+\beta)$ is designed for the plant $\frac{k}{s(s+a)}$, i.e., when the closed-loop system has the form presented in Fig. 5.29 and the open-loop transfer function is:

$$G(s)H(s) = \frac{k_d k(s+\beta)}{s(s+a)}. \tag{5.31}$$

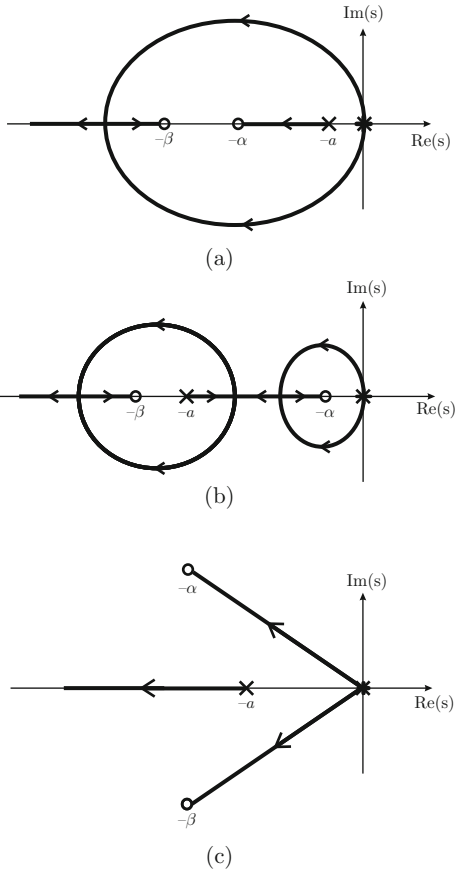

Fig. 5.28 Different possibilities for root locus diagrams of the PID control of position

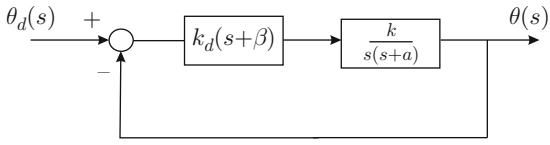

Fig. 5.29 Proportional–derivative control of the position

The closed-loop transfer function is, in this case:

$$\frac{\theta(s)}{\theta_d(s)} = \frac{k_d k(s+\beta)}{s^2 + (a + k_d k)s + k_d k\beta}.$$

Equating to a standard second-degree polynomial:

$$s^2 + (a + k_d k)s + k_d k\beta = s^2 + 2\zeta\omega_n s + \omega_n^2,$$

yields:

$$k_d = \frac{2\zeta\omega_n - a}{k}, \quad \beta = \frac{\omega_n^2}{k_d k}. \tag{5.32}$$

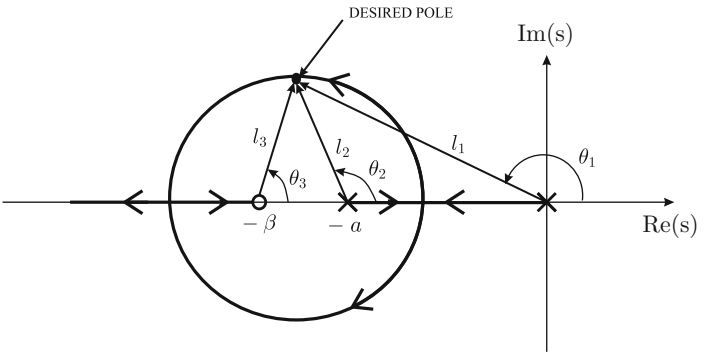

Fig. 5.30 Root locus diagram for the system in Fig. 5.29

The values for ζ and ω_n can be computed using (3.71) from the desired values for rise time and overshoot. The corresponding root locus diagram is shown in Fig. 5.30, which is identical to the case $c > a$ depicted in Fig. 5.16, because only in this case can the PD control of the position produce complex conjugate closed-loop poles. From (5.31), it is found that the angle and the magnitude conditions establish:

$$\theta_3 - (\theta_1 + \theta_2) = \pm 180^\circ(2q+1), \quad q = 1, 2, \ldots \quad \frac{k_d k l_3}{l_1 l_2} = 1, \tag{5.33}$$

where $l_1, l_2, l_3, \theta_1, \theta_2$ and θ_3 are defined in Fig. 5.30. When the factor $\frac{s+\alpha}{s}$ is included in the open-loop transfer function shown in (5.31), the resulting open-loop transfer function becomes:

$$G(s)H(s) = \frac{k_d k(s+\beta)(s+\alpha)}{s^2(s+a)}. \tag{5.34}$$

As $\alpha > 0$ is small, the corresponding root locus has the shape shown in Fig. 5.31. The reader is encouraged to follow the rules in Sect. 5.1.1 to verify this result. The angle and the magnitude conditions are established in this case from (5.34) as:

$$\theta_3 + \theta_5 - (2\theta_1 + \theta_2) = \pm 180^\circ(2q+1), \quad q = 1, 2, \ldots \quad \frac{k_d k l_3 l_5}{l_1^2 l_2} = 1, \tag{5.35}$$

where l_1, l_2, l_3, θ_1, θ_2 and θ_3 are defined as in Fig. 5.30, whereas l_5 and θ_5 are defined in Fig. 5.31. The reason for choosing $\alpha > 0$ to be close to zero is to render l_1 and l_5 almost the same such that $l_5/l_1 \approx 1$. This also ensures that θ_1 and θ_5 are almost equal; hence, $\theta_5 - \theta_1 \approx 0$. Then, the angle and the magnitude conditions in (5.33) and (5.35) are almost identical. This ensures that the closed-loop poles

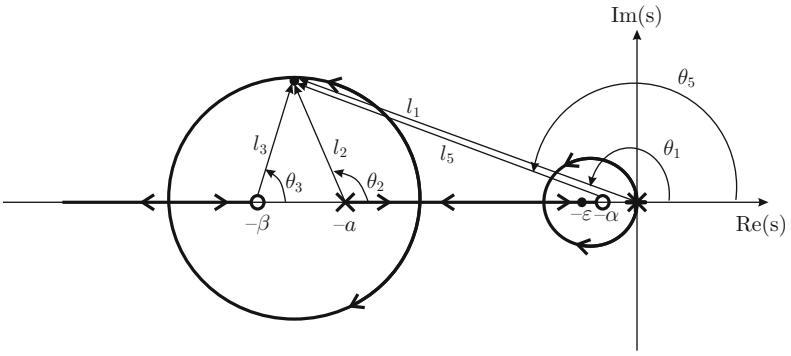

Fig. 5.31 Root locus for the open-loop transfer function shown in (5.34)

obtained when the open-loop transfer function is that presented in (5.31) are almost identical to the closed-loop poles obtained when the open-loop transfer function employed is that presented in (5.34). This ensures that the desired transient response specifications (rise time and overshoot) designed with the PD controller in (5.32) are also accomplished with the PID controller:

$$k_d \frac{(s+\alpha)(s+\beta)}{s} = k_d \frac{s^2 + \frac{k_p}{k_d} s + \frac{k_i}{k_d}}{s},$$

i.e., when the controller gains are chosen according to (5.30).

However, it is important to point out a drawback of this design approach: according to (5.30) a small α results in a small integral gain k_i. As a consequence, the deviation of the position produced by the external disturbance vanishes very slowly, which may be unacceptable in practice. This can also be explained from the root locus diagram in Fig. 5.31. Notice that a closed-loop pole (located, say, at $s = -\varepsilon$, $\varepsilon > 0$) approaches the zero at $s = -\alpha$, which means that both cancel each other out in the transfer function shown in (5.26), i.e., the effect of none of them is observed in the transient response to a reference of the position. However, the zero at $s = -\alpha$ does not appear in the transfer function shown in (5.27). But the pole at $s = -\varepsilon$ is still present in this transfer function; hence, it significantly affects the transient response: this slow pole (close to the origin) is responsible for a slow transient response when an external disturbance appears.

Despite this drawback, the traditional criteria for root locus-based design suggest proceeding as above when designing PID controllers. Moreover, it is interesting to say that these problems in traditional design methods remain without a solution despite the fact that they have been previously pointed out in some research works. See [10] for instance.

On the other hand, according to (5.30), a larger integral gain can be obtained (to achieve a faster disturbance rejection) by choosing a larger value for α. However, according to the previous discussion, this will result in a transient response to a

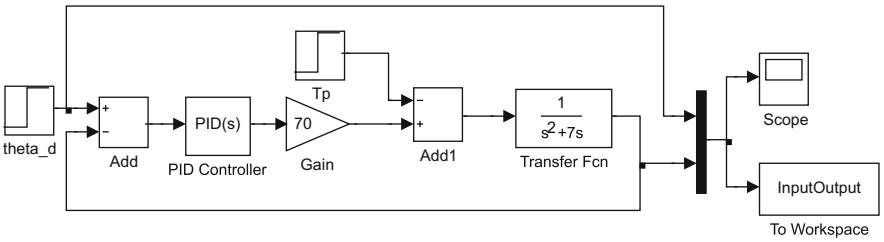

Fig. 5.32 MATLAB/Simulink diagram for the closed-loop system in Fig. 5.27a

reference of position that does not satisfy the desired specifications. Hence, it is concluded that there is no tuning rule allowing the gains of a PID controller for position to be computed exactly, simultaneously satisfying the desired transient response specifications to a given reference of the position and producing a satisfactory rejection of the effects of an external torque disturbance. These observations are experimentally verified in Chap. 11 where, given the described drawback, some new controllers solving these problems are designed and experimentally tested.

Finally, despite the above drawback, it is important to recall what was indicated just after (5.28): PID control is one of the most frequently employed controllers in industry because it can be tuned by trial and error (see Sect. 5.3). This has to be performed by taking into account the stability rule obtained in the Example 4.12, Sect. 4.3.

Example 5.5 The MATLAB/Simulink diagram corresponding to the block diagram in Fig. 5.27a is presented in Fig. 5.32. It is assumed that $a = 7$ and $k = 70$. The desired position θ_d is a step command applied at $t = 0$ with 2 as the magnitude, whereas the disturbance T_p is another step applied at $t = 0.5$[s] and 700 as the magnitude. The PID controller gains are k_p, k_d, and k_i, computed in the following MATLAB code executed in an m-file:

```
clc
a=7;
k=70;
tr=0.05;
Mp=14;%
z=sqrt( log(Mp/100)^2 /( log(Mp/100)^2 + pi^2 ) );
wn=1/(tr*sqrt(1-z^2))*(pi-atan(sqrt(1-z^2)/z));
s=-z*wn+wn*sqrt(1-z^2)*j
kd=(2*z*wn-a)/k;
beta=wn^2/(k*kd)
den1=conv([1 -s],[1 -real(s)+j*imag(s)]);
Md=tf(den1(3),den1);
gm=tf(k,[1 a 0]);
PD=tf(kd*[1 beta],1);
alpha=20;%0.1 1 10 20
```

```
PI=tf([1 alpha],[1 0]);
M_pid=feedback(PI*PD*gm,1,-1);
pole(M_pid)
figure(2)
step(Md*2,'r--',M_pid*2,'k--',0.25)
hold on
kp=(alpha+beta)*kd;
ki=alpha*beta*kd;
%%{
nn=length(InputOutput(:,2));
n=nn-1;
Ts=2/n;
t=0:Ts:2;
figure(3)
plot(t,InputOutput(:,2),'k--');
hold on
plot(t,InputOutput(:,1),'k:');
axis([0 1 0 3])
xlabel('t [s]')
ylabel('theta [rad]')
%}
```

The main idea is to propose different values for the design parameter α to see how the transient response is affected. Hence, the values for ζ and ω_n are first computed from the desired rise time $t_r = 0.05$[s] and overshoot $M_p = 14\%$. This allows k_d and β to be computed using (5.32). Then, the desired time response, i.e., that dictated by the desired complex conjugate poles at $s = -z * wn \pm wn * sqrt(1 - z^2)j$ (the slowest dashed response in Fig. 5.33), and the actual closed-loop system response to the step reference are plotted on the same axes using the command "$step(Md * 2,' r - -', M\_pid * 2,' k - -', 0.25)$". The proportional and integral gains are computed using (5.30); hence, the simulation in Fig. 5.32 can be run. Once this is performed, the remaining commands in the code listed above can be used to draw Fig. 5.34.

Running the above code and the simulation in Fig. 5.32 several times, the responses are obtained when using different values for α. In Figs. 5.33 and 5.34: (i) Continuous lines stand for $\alpha = 0.1$, (ii) Dash–dot: $\alpha = 1$, (iii) Dotted: $\alpha = 10$, and the fastest dashed line: $\alpha = 20$.

It is observed that, when $\alpha = 0.1$, the response is different from the desired one, i.e., the slowest dashed line in Fig. 5.33. This is because of the closed-loop zero at $-\beta$, located at $s = -54.5225$ in this case, which deviates the system response from the desired one (See also Fig. 5.20. It is remarked that the desired closed-loop poles are located at $s = -\zeta\omega_n \pm j\omega_n\sqrt{1-\zeta^2}$, as desired, in this case. Also notice that the disturbance rejection is so slow that it seems that a steady-state deviation might exist.

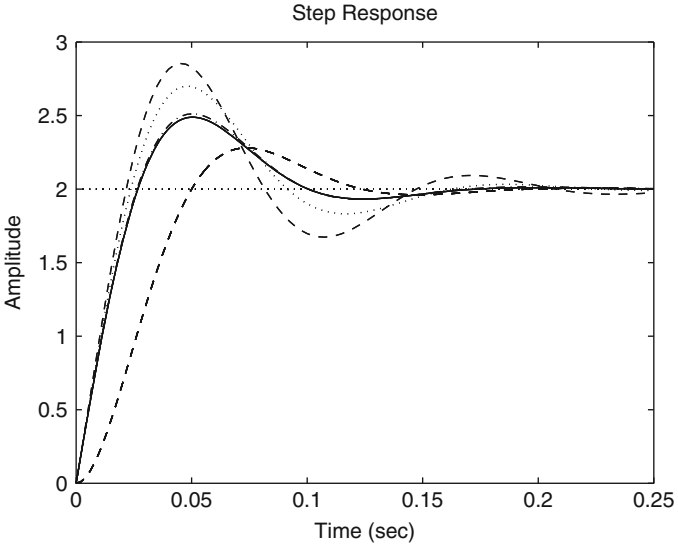

Fig. 5.33 Response to a step command in the desired position $\theta_d(s)$

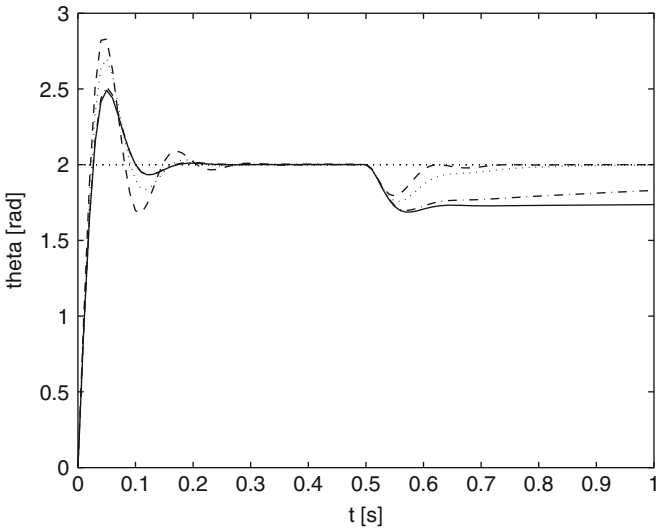

Fig. 5.34 Response to a step disturbance $T_p(s)$

As α is chosen to be larger, the performance observed in Fig. 5.34 improves with respect to the disturbance rejection, but the price to be paid is that the response to the position reference is increasingly different from the desired one, as observed in Fig. 5.33.

Thus, the simulation results in this example corroborate the predictions stated in the above discussion in the present section.

5.2.6 Assigning the Desired Closed-Loop Poles

An example is presented in this section to show how the root locus method can be used to assign the desired closed-loop poles. Consider the following transfer function:

$$G(s)H(s) = \frac{k}{(s - 35.7377)(s + 36.5040)}. \tag{5.36}$$

The gain k is varied by the method to take values from 0 to $+\infty$. First, $G(s)H(s)$ is rewritten as:

$$G(s)H(s) = \frac{k}{l_1 l_2} \angle -(\theta_1 + \theta_2),$$

where the vectors $s - 35.7377 = l_1 \angle \theta_1$ and $s - (-36.5040) = l_2 \angle \theta_2$ have been defined. The fundamental conditions in the root locus method are the angle condition (5.7) and the magnitude condition (5.6), which are expressed respectively as:

$$-(\theta_1 + \theta_2) = \pm(2q + 1)180^\circ, \quad q = 0, 1, 2, \ldots$$
$$\frac{k}{l_1 l_2} = 1.$$

Rule 5 indicates that the root locus on the real axis only exists between the points $s = 35.7377$ and $s = -36.5040$. Moreover, according to rule 1, the root locus begins ($k = 0$) at $s = 35.7377$ and $s = -36.5040$. On the other hand, according to rules 2 and 3, when k tends to $+\infty$ the branches starting at $s = 35.7377$ and $s = -36.5040$ must end at some open-loop zero (there is no zero in this case) or at some point at infinity on the s plane. Hence, the root locus must move away from the points $s = 35.7377$ and $s = -36.5040$ on the real axis as k increases and a breakaway point must exist somewhere between such points. Then, the branches must move toward infinity on the s plane.

On the other hand, according to the angle condition, to $-(\theta_1 + \theta_2) = -180^\circ = -(\alpha + \theta_1)$, and to Fig. 5.35, it can be observed that $\alpha = \theta_2$; hence, the triangles t_1 and t_2 must be identical for any closed-loop pole s. Then, both branches, which are also shown in Fig. 5.35, must be parallel to the imaginary axis. This means that the breakaway point on the real axis is located at the middle point between $s = 35.7377$ and $s = -36.5040$, i.e., at $(35.7377 - 36.5040)/2 = -0.7663$. This can also be verified using rules 3 and 4. Finally, according to rule 6, both branches are symmetrical with respect to the real axis.

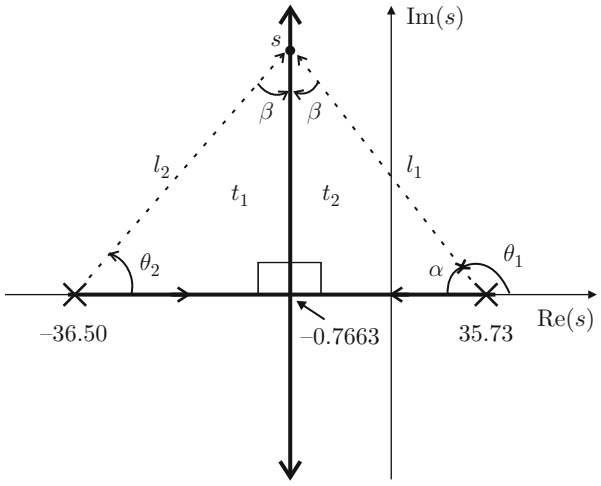

Fig. 5.35 Root locus for $G(s)H(s)$ in (5.36)

The magnitude condition is employed when it is required to know the exact value of k rendering a specific point on the root locus an actual closed-loop pole. Notice, for instance, that both l_1 and l_2 must increase to satisfy the magnitude condition as k grows to $+\infty$:

$$\frac{k}{l_1 l_2} = 1,$$

which means that the closed-loop poles corresponding to large values of k tend toward some points at infinity on the s plane.

Now suppose that an additional pole is included in the transfer function in (5.36) to obtain:

$$\begin{aligned} G(s)H(s) &= \frac{116137\,k}{s^3 + 72.54s^2 - 1250s - 9.363 \times 10^4}, \\ &= \frac{116137\,k}{(s - 35.7377)(s + 36.5040)(s + 71.7721)}. \end{aligned} \tag{5.37}$$

Again, k is the gain that the method varies from 0 to $+\infty$ to plot the root locus diagram. First, $G(s)H(s)$ is rewritten as:

$$G(s)H(s) = \frac{116137\,k}{l_1 l_2 l_3} \angle -(\theta_1 + \theta_2 + \theta_3),$$

where the vectors $s - 35.7377 = l_1 \angle \theta_1$, $s - (-36.5040) = l_2 \angle \theta_2$, and $s - (-71.7721) = l_3 \angle \theta_3$ have been defined. The angle condition (5.7) and the magnitude condition (5.6) are expressed respectively as:

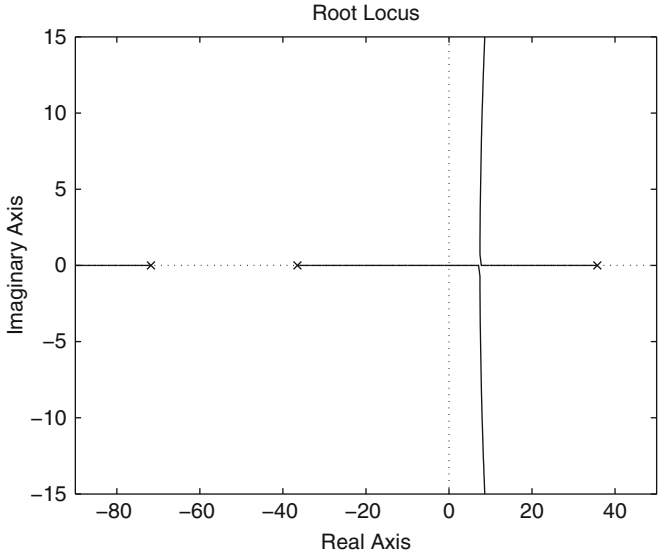

Fig. 5.36 Root locus diagram for $G(s)H(s)$ in (5.37)

$$-(\theta_1+\theta_2+\theta_3)=\pm(2q+1)180^\circ, \quad q=0,1,2,\ldots$$
$$\frac{116137\,k}{l_1 l_2 l_3}=1.$$

The root locus diagram corresponding to this case can be obtained from the root locus diagram obtained for the transfer function in (5.36) by simply taking into account the additional pole at $s=-71.7721$.

According to the rule 11, the new pole is responsible for both branches of the root locus shown in Fig. 5.35 bending to the right, as can be observed in Fig. 5.36. This can be corroborated using rule 3 to find that, now, three branches exist, which tend toward the asymptotes at $\pm 180^\circ$ and $\pm 60^\circ$ with respect to the positive real axis.

On the other hand, the breakaway point between the points $s=35.7377$ and $s=-36.5040$, which was located at $(35.7377-36.5040)/2=-0.7663$ in Fig. 5.35, is now shown in Fig. 5.36 shifted to the right of -0.7663. The reason for this is explained in Fig. 5.37 where s' and s stand for the points on the root locus which are very close to the breakaway point for the case of Figs. 5.35 and 5.36 respectively. As $-(\theta_1+\theta_2+\theta_3)=-180^\circ$ must be satisfied in Fig. 5.36, whereas $-(\theta_1'+\theta_2')=-180^\circ$ must be satisfied in Fig. 5.35, then both θ_1 and θ_2 must be smaller than θ_1' and θ_2'. This means that the point s must be shifted to the right of the point s'. Notice that this displacement of the breakaway point to the right of the point -0.7663 is greater as the angle θ_3 introduced by the pole at $s=-71.7721$ is greater, i.e., as this pole is placed farther to the right. In fact, it is observed in Fig. 5.36 that the breakaway point is located on the right half-plane.

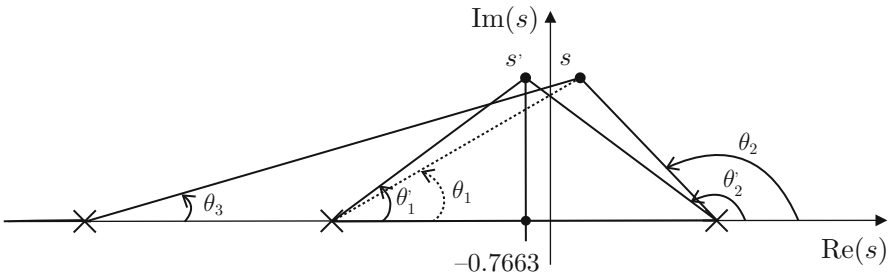

Fig. 5.37 An additional pole moves the breakaway point to the right

This description of the root locus diagram in Fig. 5.36 allows us to conclude that there is always at least one closed-loop pole with a positive real part, i.e., the closed-loop system is unstable for any positive value of k. As k can be interpreted as the gain of a proportional controller, it is concluded that it is not possible to render the closed-loop system stable using any proportional controller and, thus, another controller must be proposed. According to rule 12 it is required to use a controller introducing an open-loop zero because this bends the root locus to the left accomplishing closed-loop stability.

Consider the following open-loop transfer function:

$$\begin{aligned} G(s)H(s) &= k\frac{116137(s+b)}{s^3+72.54s^2-1250s-9.363\times 10^4}, \\ &= k\frac{116137(s+b)}{(s-35.7377)(s+36.5040)(s+71.7721)}, \end{aligned} \tag{5.38}$$

with b a positive constant. Again, k is the gain that the method varies from 0 to $+\infty$ to draw the root locus diagram. First, $G(s)H(s)$ is rewritten as:

$$G(s)H(s) = \frac{116137\ k\ l_4}{l_1 l_2 l_3}\angle[\theta_4 - (\theta_1+\theta_2+\theta_3)], \tag{5.39}$$

where the vectors $s-35.7377 = l_1\angle\theta_1$, $s-(-36.5040) = l_2\angle\theta_2$, $s-(-71.7721) = l_3\angle\theta_3$, and $s-(-b) = l_4\angle\theta_4$ have been defined. The angle condition (5.7) and the magnitude condition (5.6) are expressed respectively as:

$$\theta_4 - (\theta_1+\theta_2+\theta_3) = \pm(2q+1)180^\circ, \quad q = 0, 1, 2, \ldots \tag{5.40}$$

$$\frac{116137\ k\ l_4}{l_1 l_2 l_3} = 1. \tag{5.41}$$

Notice that, now, $n = 3$, $m = 1$, $p_1 = 35.7377$, $p_2 = -36.5040$, $p_3 = -71.7721$, and $z_1 = -b$. According to the rules 1, 2, and 3, one of the three branches starting ($k = 0$) at the points $s = 35.7377$, $s = -36.5040$, and $s = -71.7721$ (the open-

loop poles) must end ($k = +\infty$) at the open-loop zero $s = -b$. Hence, there are two root locus branches tending toward some points at infinity of the s plane. According to rule 3, the angles of the asymptotes toward which these branches tend are:

$$\frac{\pm 180^\circ(2 \times 0 + 1)}{n - m} = \frac{\pm 180^\circ(2 \times 0 + 1)}{3 - 1} = \pm 90^\circ.$$

Moreover, according to rule 4, the point where these asymptotes cross the real axis can be shifted by using the zero at $s = -b$:

$$\sigma_a = \frac{p_1 + p_2 + p_3 - (-b)}{n - m} = \frac{35.7377 - 36.5040 - 71.7721 + b}{2}. \quad (5.42)$$

Notice that b must be positive, as, if this is not the case, the root locus would be pushed to the right half-plane producing unstable closed-loop poles. Also notice that the asymptotes move to the left (increasing stability) as the zero is located closer to the origin, i.e., as b tends toward zero. This means that the closed-loop poles cannot be placed arbitrarily to the left.

According to rule 5, the root locus now exists on two segments of the real axis. The locations of these segments depend on the value of b as shown in Figs. 5.38a and b. Furthermore, it is shown in Fig. 5.38c that in the case when $b = 36.5040$ is selected, the open-loop zero at $s = -b$ cancels with the open-loop pole at $s = -36.5040$. This means that, in such a case, the root locus only exists in one segment on the real axis.

It is observed, in Fig. 5.38c, that only two closed-loop poles exist. It is observed, in Figs. 5.38a and b, that three closed-loop poles exist and one of them is on the right half-plane (closed-loop instability) if the gain k is too small. On the other hand, if k is too large, two complex conjugate poles exist with too large an imaginary part, i.e., producing a fast oscillation. Although in theory this can work because the three poles have negative real parts, a large k produces a number of practical problems such as noise amplification and power amplifier saturation, i.e., the control system may not work correctly in practice. Hence, a good design is that enabling the designer to locate as desired the closed-loop poles avoiding the use of values that are too large and values that are too small for the gain k.

Suppose that $s = -25 \pm j40$ are the desired closed-loop complex conjugate poles. A procedure that is useful for computing the exact values required for both b and k is presented in the following. According to Fig. 5.39 the following angles are computed:

$$\theta_3 = \arctan\left(\frac{40}{71.7721 - 25}\right),$$

$$\theta_2 = \arctan\left(\frac{40}{36.5040 - 25}\right),$$

$$\theta_1 = 180^0 - \arctan\left(\frac{40}{35.7377 + 25}\right).$$

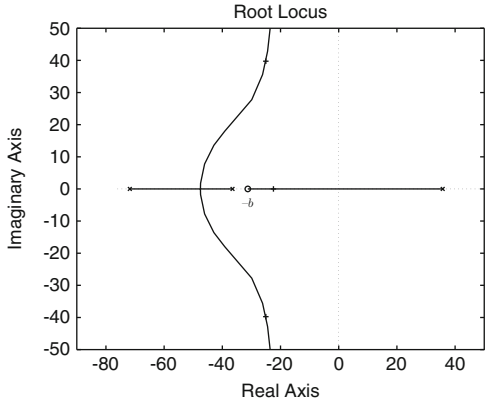

(a)

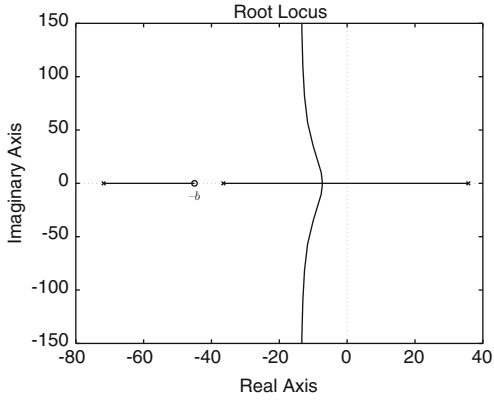

(b)

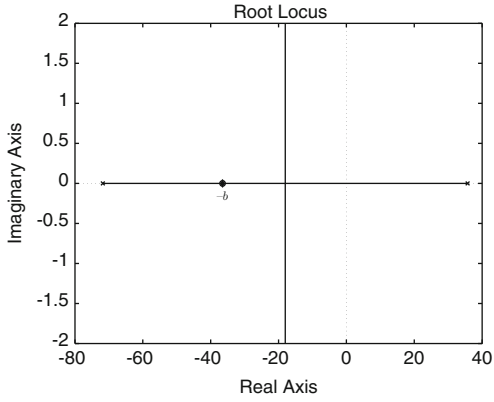

(a)

Fig. 5.38 Root loci for $G(s)H(s)$ defined in (5.38) obtained by changing b . (**a**) $b = 31.24 < 36.50$. (**b**) $b > 36.50$. (**c**) $b = 36.50$

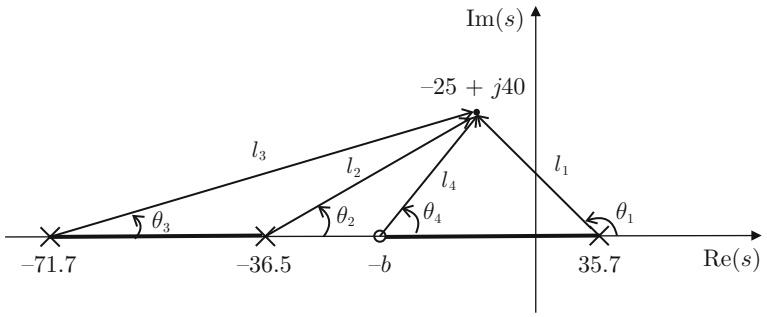

Fig. 5.39 Open-loop poles and zeros when trying to locate the desired closed-loop poles at $s = -25 \pm j40$

Using the angle condition (5.40), θ_4 is computed and, also, b:

$$\theta_4 = -180^0 + (\theta_1 + \theta_2 + \theta_3),$$
$$b = \frac{40}{\tan(\theta_4)} + 25 = 31.2463.$$

On the other hand, according to Fig. 5.39, the following lengths are computed:

$$l_4 = \sqrt{40^2 + (b - 25)^2},$$
$$l_3 = \sqrt{40^2 + (71.7721 - 25)^2},$$
$$l_2 = \sqrt{40^2 + (36.5040 - 25)^2},$$
$$l_1 = \sqrt{40^2 + (35.7377 + 25)^2},$$

and, finally, the magnitude condition (5.41) is employed to compute k:

$$k = \frac{l_1 l_2 l_3}{116137\, l_4} = 0.0396.$$

The location of the third closed-loop pole can be found from the condition $1 + G(s)H(s) = 0$ using $G(s)H(s)$ given in (5.38) and $b = 31.2463$ and $k = 0.0396$, i.e.,

$$1 + 0.0396 \frac{116137(s + 31.2463)}{s^3 + 72.54s^2 - 1250s - 9.363 \times 10^4} = 0, \tag{5.43}$$

hence:

$$s^3 + 72.54s^2 + (0.0396 \times 116137 - 1250)s$$
$$+(0.0396 \times 116137 \times 31.2463 - 9.363 \times 10^4) = 0.$$

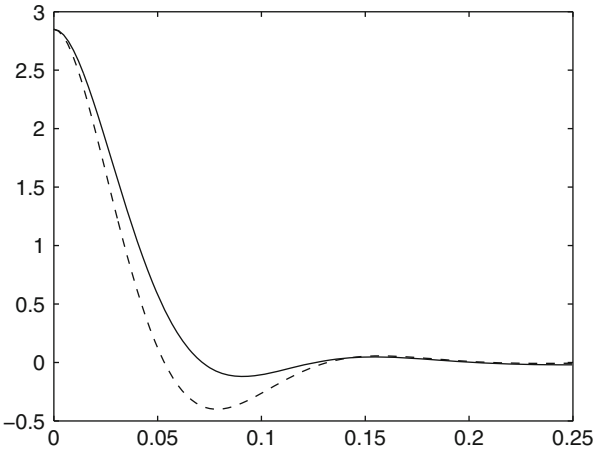

Fig. 5.40 Closed-loop response of the system (5.38) from an initial output that is different from zero. Continuous line: designed response. Dashed line: desired response. Vertical axis: y[m]. Horizontal axis: time in seconds

The roots of this polynomial are the closed-loop poles when $b = 31.2463$ and $k = 0.0396$. Using MATLAB, it is found that these roots are $-25.0037 + j39.9630$, $-25.0037 - j39.9630$ and -22.5326. These poles are also shown in Fig. 5.38a using symbols "+." Notice that the desired complex conjugate poles have been successfully assigned and the third pole, which is real, is also located on the left half-plane, i.e., closed-loop stability has been accomplished. Recall that the factor $k(s + b)$ represents a PD controller.

It is important to say that this control system is employed to regulate the output at a zero value. This implies that no matter what the system type, the desired output (i.e., zero) is reached. Hence, consideration with respect to the steady-state response is not necessary.

The closed-loop response (continuous line) is shown in Fig. 5.40 when the desired output is zero, $r = 0$ (see Fig. 5.1). In this simulation (5.38), $b = 31.2463$ and $k = 0.0396$ are employed. The dashed line represents the response of a system with the transfer function $\frac{\omega_n^2}{s^2+2\zeta\omega_n s+\omega_n^2}$ whose poles are located at $s = -25 \pm j40$. Thus, this system represents what is known as a reference model, because its response possesses the desired transient response specifications. Both responses start from an initial output equal to 2.85. Notice that some differences exist between these responses, which are due to the zero at $s = -31.2463$ and the closed-loop pole at $s = -22.5326$, because they are not close enough to completely cancel out their effects.

Finally, Figs. 5.36, 5.38 and 5.40 have been drawn using the following MATLAB code in an m-file:

```
clc
clear
```

```
gh=tf(116137,[1 72.54 -1250 -9.363e4]);
figure(1)
rlocus(gh)
axis([-90 50 -15 15])
b=31.24;
gh=tf(116137*[1 b],[1 72.54 -1250 -9.363e4]);
figure(2)
rlocus(gh)
axis([-90 50 -50 50])
b=45;
gh=tf(116137*[1 b],[1 72.54 -1250 -9.363e4]);
figure(3)
rlocus(gh)
axis([-80 40 -150 150])
b=36.5;
gh=tf(116137*[1 b],[1 72.54 -1250 -9.363e4]);
figure(4)
rlocus(gh)
axis([-80 40 -2 2])
b=31.2463;
k=0.0396;
gh=tf(116137*k*[1 b],[1 72.54 -1250 -9.363e4]);
M=feedback(gh,1,-1)
A=[0 1 0;
0 0 1;
-5.007e4 -3349 -72.54];
B=[0;
0;
1];
C=[1.437e5 4599 0];
Me=ss(A,B,C,0);
dend=conv([1 25+40*j],[1 25-40*j]);
Ad=[0 1;
-dend(3) -dend(2)];
Bd=[0;
dend(3)];
Cd=[1 0];
Md=ss(Ad,Bd,Cd,0);
figure(5)
initial(Me,'b-',[2.8/1.437e5 0 0])
hold on
initial(Md,'r--',[2.8 0])
```

5.2.7 Proportional–Integral–Derivative Control of an Unstable Plant

In this section, the use of the root locus method to select the gains of a PID controller for an open-loop unstable plant is presented. The open-loop transfer function is:

$$G(s)H(s) = \frac{11613700\, k_d}{s^3 + 2739s^2 - 1250s - 3.536 \times 10^6} \left(\frac{s^2 + \frac{k_p}{k_d} s + \frac{k_i}{k_d}}{s} \right) \quad (5.44)$$

where k_d is the parameter that the method varies from 0 to $+\infty$ to draw the root locus, whereas $\frac{k_p}{k_d}$ and $\frac{k_i}{k_d}$ must be proposed. Notice that a PID controller is selected because it renders the system type 1, i.e., to ensure a zero steady-state error when the desired output is a constant. Notice that the PID controller introduces two open-loop zeros. There are four open-loop poles placed at:

$$s_1 = 35.9, \qquad s_2 = -2739.4, \qquad s_3 = -35.9, \quad s_4 = 0.$$

Using rule 3 it is found that there are $n - m = 4 - 2 = 2$ branches of the root locus that tend toward infinity on the plane s following the asymptotes whose angles are given as:

$$\frac{\pm 180^\circ}{2} = \pm 90^\circ.$$

Moreover, according to rule 4, the point on the real axis where these asymptotes intersect is:

$$\sigma_a = \frac{35.9 - 2739.4 - 35.9 + \sigma_{z1} + \sigma_{z2}}{2},$$

where $-\sigma_{z1} < 0$ and $-\sigma_{z2} < 0$ are the real parts of both open-loop zeros introduced by the PID controller (these values have to be proposed). It is clear that σ_a moves to the left (which implies that the closed-loop system becomes more stable) if $-\sigma_{z1} < 0$ and $-\sigma_{z2} < 0$ are chosen to be close to zero. Notice that this is in agreement with rule 12. Thus, it is concluded that $\sigma_a < -1100$ is placed far to the left of the origin. Using these observations, in addition to rules 1, 2, 5, and 6, it is found that the root locus has the three possibilities depicted in Fig. 5.41.

Instead of assigning some desired closed-loop poles, the control objective is simply to render the closed-loop system stable. As previously stated, it is preferable to place both open-loop zeros close to the origin. This means that the possibility shown in Fig. 5.41a is to be used. On the other hand, two complex conjugate zeros would force two complex conjugate closed-loop poles to appear, which would result in a less damped closed-loop system. It is for this reason that the possibility in Fig. 5.41c is also avoided. Hence, searching for a root locus diagram such as that in

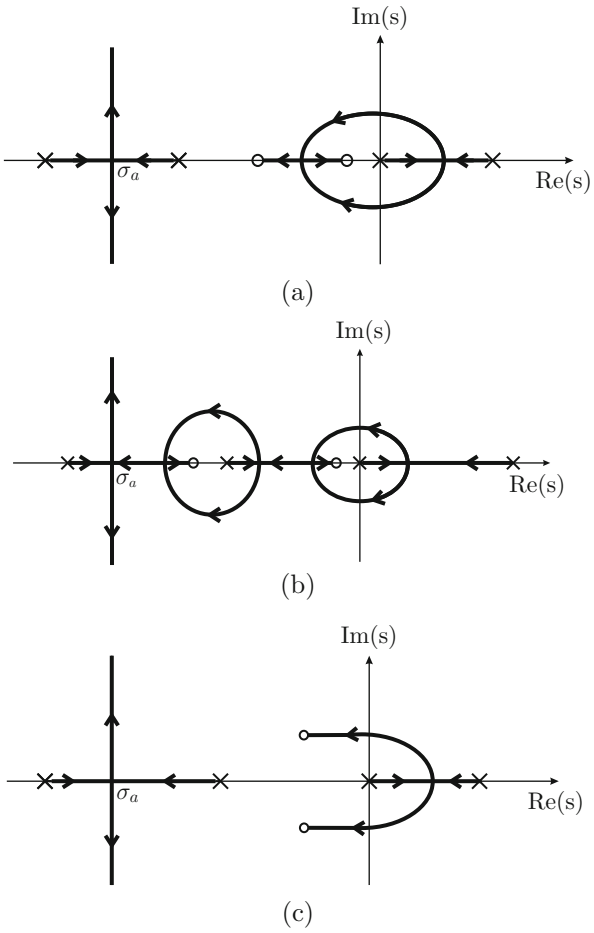

Fig. 5.41 Different possibilities for the root locus diagram when using (5.44) as the open-loop transfer function

Fig. 5.41a, the following values are proposed:

$$\frac{k_p}{k_d} = 31.24, \quad \frac{k_i}{k_d} = \frac{31.24}{0.8}, \tag{5.45}$$

as this assigns two open-loop zeros at:

$$s_5 = -29.9355, \quad s_6 = -1.3045,$$

i.e., they are located between the open-loop poles at:

$$s_3 = -35.9, \quad s_4 = 0.$$

The facts that $\sigma_a < -1100$ is located far to the left of the origin and that the asymptotes form $\pm 90^\circ$ angles, ensure that a minimal k_d exists for all closed-loop poles to be placed on the left half-plane. Using (5.45) and Routh's criterion, it is found that:

$$k_d > 0.01, \tag{5.46}$$

ensures that all of the closed-loop poles are located on the left half-plane and, hence, the closed-loop system is stable. This is performed as follows. From the condition $1 + G(s)H(s) = 0$, i.e., using (5.44) and (5.45), the following characteristic polynomial is obtained:

$$\begin{aligned} &s^4 + a_3 s^3 + a_2 s^2 + a_1 s + a_0 = 0, \\ &a_3 = 2739, \quad a_2 = 11613700\, k_d - 1250, \\ &a_1 = 11613700 \times 31.24\, k_d - 3.536 \times 10^6, \\ &a_0 = 11613700 \times \frac{31.28}{8}\, k_d. \end{aligned} \tag{5.47}$$

To apply Routh's criterion, the Table 5.1 is filled. Closed-loop stability is ensured if no sign changes exist in the first column of Table 5.1, i.e., if:

$$\frac{a_3 a_2 - a_1}{a_3} > 0, \quad \frac{e a_1 - a_3 a_0}{e} > 0, \quad a_3 > 0, \quad a_0 > 0. \tag{5.48}$$

Notice that the third condition in (5.48) is naturally satisfied and from the first and the last conditions it is found that:

$$k_d > -3.5695 \times 10^{-6}, \quad k_d > 0. \tag{5.49}$$

From the second condition in (5.48) the following is found:

$$\begin{aligned} &k_d^2 + \left(\frac{b_1}{b_2} - \frac{b_3}{b_4} - 2739^2 \frac{b_5}{b_2 b_4} \right) k_d - \frac{b_1 b_3}{b_2 b_4} > 0, \\ &b_1 = 112250, \quad b_2 = 3.1447 \times 10^{10}, \quad b_3 = 3.536 \times 10^6, \\ &b_4 = 11613700 \times 31.24, \quad b_5 = 11613700 \frac{31.28}{8}. \end{aligned} \tag{5.50}$$

Table 5.1 Applying Routh's criterion to the polynomial in (5.47)

s^4	1	a_2	a_0
s^3	a_3	a_1	0
s^2	$\frac{a_3 a_2 - a_1}{a_3} = e$	a_0	0
s^1	$\frac{e a_1 - a_3 a_0}{e}$	0	
s^0	a_0		

It is not difficult to find that the roots of the second-degree polynomial in (5.50) are $k_d = 0.01$ and $k_d = -3.5 \times 10^{-6}$. Moreover, it is possible to evaluate numerically to find that:

$$\begin{aligned}
&(k_d - 0.01)(k_d + 3.5 \times 10^{-6}) > 0, \quad \text{if } k_d < -3.5 \times 10^{-6},\\
&(k_d - 0.01)(k_d + 3.5 \times 10^{-6}) < 0, \quad \text{if } -3.5 \times 10^{-6} < k_d < 0.01,\\
&(k_d - 0.01)(k_d + 3.5 \times 10^{-6}) > 0, \quad \text{if } k_d > 0.01.
\end{aligned}$$

Thus, to simultaneously satisfy (5.49) and (5.50), i.e., to ensure closed-loop stability, (5.46) must be chosen.

Example 5.6 The root locus diagram for $G(s)H(s)$ given in (5.44) under the conditions in (5.45) is shown in Fig. 5.42. This has been obtained using the following MATLAB code in an m-file.

```
clc
clear
gh=tf(11613700*[1 31.24 31.24/0.8],[1 2739 -1250
 -3.536e6 0]);
k=0:0.00001:0.1;
figure(1)
rlocus(gh,k)
axis([-70 50 -10 10])
rlocfind(gh)
%%{
M=feedback(0.0226*gh,1,-1)
A=[0 1 0 0;
0 0 1 0;
0 0 0 1;
-1.025e007 -4.664e006 -2.612e005 -2739];
B=[0;
0;
0;
1];
C=[1.025e007 8.2e006 2.625e005 0];
Me=ss(A,B,C,0);
figure(2)
initial(Me,'b-',[1/1.025e007 0 0 0])
axis([-0.1 3 -0.8 1.2])
%}
```

Using the command "rlocfind(gh)", the closed-loop poles on the imaginary axis have been selected to find that $k_d = 0.01$, which corroborates the above findings, i.e., see (5.46). Using the command "pole(M)," all the closed-loop poles were found to be real, located at $s = -2640$, $s = -75.6$, $s = -20.1$, and $s = -2.6$ when

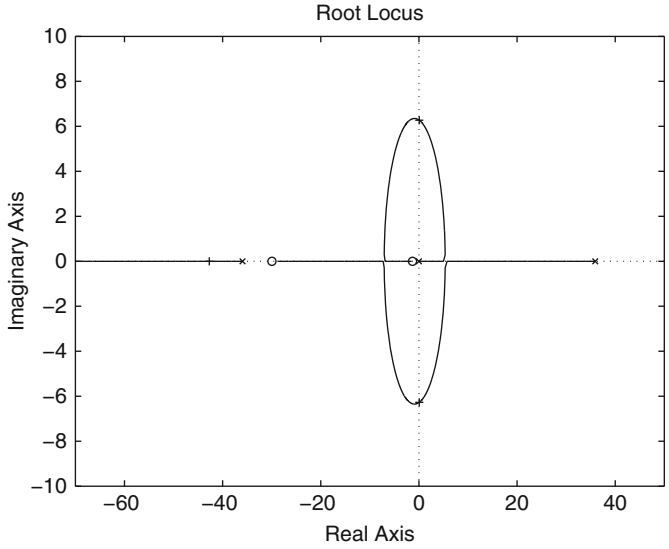

Fig. 5.42 Root locus diagram for $G(s)H(s)$ given in (5.44) under the conditions in (5.45)

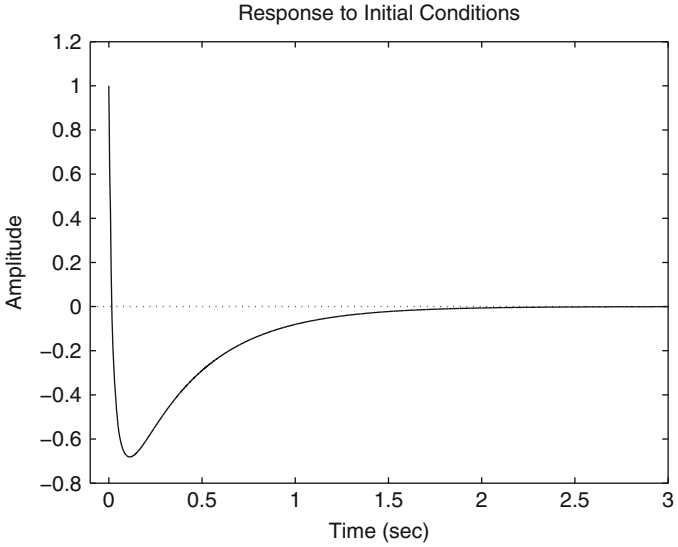

Fig. 5.43 Closed-loop time response when $G(s)H(s)$ is given in (5.44) under the conditions in (5.45) and $k_d = 0.0226$

$k_d = 0.0226$, i.e., the closed-loop system is stable. Notice that the open-loop zeros are located at $s = -29.93$ and $s = -1.3$, which was found using the command "zero(gh)." This means that all the closed-loop poles are located on the left of the open-loop zero at $s = -1.3$. Hence, according to Sect. 8.1.2, this means that

overshoot is unavoidable despite the fact that all the closed-loop poles are real. This explains the large overshoot observed in Fig. 5.43, when a zero reference is commanded and the initial output is 1. Thus, in this example, it is not important to try to assign the closed-loop poles at some specific locations.

5.2.8 *Control of a Ball and Beam System*

In this section, a controller is designed for the ball and beam system that is built and experimentally tested in Chap. 14, Sect. 14.9. Assume that a proportional controller is proposed with gain γ. First, one proceeds to study the possibility that the closed-loop system might be rendered stable for some positive gain γ. The other system parameters are positive too, but they cannot be changed. The corresponding block diagram is shown in Fig. 5.44. The open-loop transfer function is:

$$\frac{X(s)}{X_d(s)} = \frac{\gamma A_x k\rho}{s^4 + as^3 + \gamma A_x k\rho},$$
$$A_x = 5.3750, \quad k = 16.6035, \quad a = 3.3132, \quad \rho = 5.$$

The stability of the closed-loop system is studied using Routh's criterion. Thus, Table 5.2 is filled using the closed-loop characteristic polynomial $s^4+as^3+\gamma A_x k\rho$. Notice that one entry at the first column is zero; hence, the method suggests replacing it by a small $\varepsilon > 0$. Also notice that under this condition, there are two sign changes in the first column of Table 5.2 and this cannot be modified by adjusting $\gamma > 0$. Then, it is concluded that no proportional controller exists to render the closed-loop system stable. Thus, another controller must be proposed.

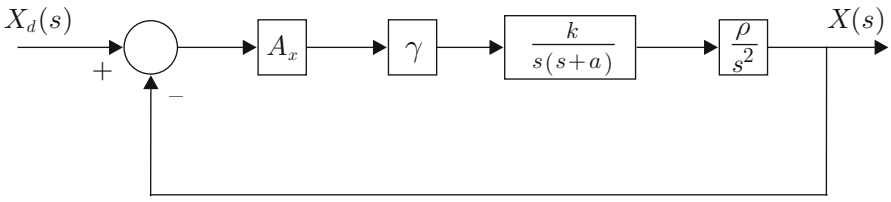

Fig. 5.44 Closed-loop system. Proportional control with gain γ

Table 5.2 Applying Routh's criterion to the polynomial $s^4 + as^3 + \gamma A_x k\rho$

s^4	1	0	$\gamma A_x k\rho$
s^3	a	0	0
s^2	$0 \approx \varepsilon$	$\gamma A_x k\rho$	
s^1	$\frac{-a\gamma A_x k\rho}{\varepsilon}$	0	
s^0	$\gamma A_x k\rho$		

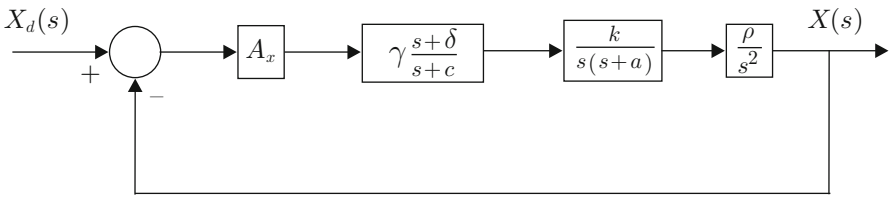

Fig. 5.45 Closed-loop system. Use of a lead compensator

According to rule 12 in Sect. 5.1.1, a PD controller can render closed-loop stable system an open-loop unstable system because a PD controller introduces an open-loop zero. However, a PD controller amplifies noise because of the derivative action. This is clearly shown in Chap. 6 where a PD controller is proved to be a high-pass filter and noise is a high-frequency signal. One way of maintaining the stabilizing properties of a PD controller, but reducing the effects of noise is to use a lead compensator, i.e., a controller with the transfer function $\gamma\frac{s+\delta}{s+c}$ with $c > \delta > 0$. It is for this reason that we study the possibility of stabilizing the ball and beam system using the block diagram in Fig. 5.45 in the following. The closed-loop transfer function is:

$$\frac{X(s)}{X_d(s)} = \frac{\gamma A_x k\rho(s+\delta)}{s^5 + (a+c)s^4 + acs^3 + \gamma A_x k\rho s + \gamma A_x k\rho\delta}.$$

The closed-loop stability is studied using Routh's criterion. Hence, the Table 5.3 is constructed using the closed-loop characteristic polynomial $s^5 + (a+c)s^4 + acs^3 + \gamma A_x k\rho s + \gamma A_x k\rho\delta$. As all the parameters are positive, there are at least two sign changes in the first column of Table 5.3. Then, it is concluded that there is no lead compensator rendering the closed-loop system stable; thus, another control strategy must be proposed. Carefully analyzing Table 5.3, it is concluded that the problem is originated by the first entry corresponding to row s^2, i.e., $\frac{-(a+c)e}{ac}$, which is negative. Notice that this is a consequence of the fact that the second entry in the row corresponding to s^4 is equal to zero. This is because s^2 has a zero coefficient in the polynomial $s^5+(a+c)s^4+acs^3+\gamma A_x k\rho s+\gamma A_x k\rho\delta$. Thus, it is concluded that the closed-loop system may be rendered stable if the characteristic polynomial of the open-loop transfer function has a positive coefficient for s^2. Next, it is shown that this is possible if two internal loops are employed, as shown in Fig. 5.46. Notice that a lead compensator is still considered. In this case, the open-loop transfer function is given as:

$$G(s)H(s) = \frac{A_x\ \rho\ \gamma}{A_\theta}\ \frac{s+b}{s+c}\ \frac{\alpha k A_\theta}{s^2 + (a + k_v k A_\theta)s + \alpha k A_\theta}\ \frac{1}{s^2}, \qquad (5.51)$$

$$c > b > 0, \quad \gamma > 0, \quad A_\theta = 0.9167.$$

Table 5.3 Applying Routh's criterion to polynomial $s^5 + (a+c)s^4 + acs^3 + \gamma A_x k\rho s + \gamma A_x k\rho\delta$

s^5	1	ac	$\gamma A_x k\rho$
s^4	$a+c$	0	$\gamma A_x k\rho\delta$
s^3	ac	$\frac{(a+c)\gamma A_x k\rho - \gamma A_x k\rho\delta}{a+c} = e$	
s^2	$\frac{-(a+c)e}{ac} = f$	$\gamma A_x k\rho\delta$	
s^1	$\frac{fe - ac\gamma A_x k\rho\delta}{f}$	0	
s^0	$\gamma A_x k\rho\delta$		

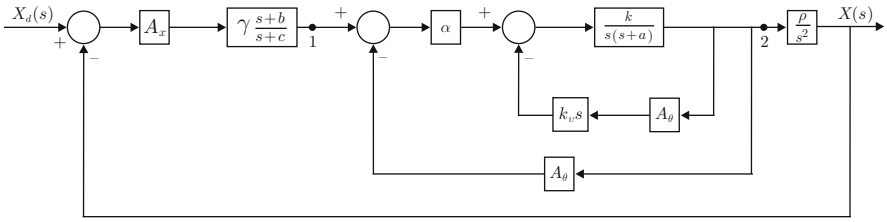

Fig. 5.46 Closed-loop system. Use of two internal loops and a lead compensator

Notice that the system type is 2, i.e., the steady state error is zero if the reference is a step or a ramp. The reader may obtain the closed-loop transfer function $\frac{X(s)}{X_d(s)}$ to verify that the corresponding characteristic polynomial has degree 5 and all of its coefficients are positive (including the coefficient of s^2), as expected. According to the previous discussion, this means that there exists the possibility of finding positive values for γ, c, b (with $c > b$), k_v and α such that the closed-loop system is stable. These values are found in the following using the root locus method.

Suppose that the roots of the polynomial $s^2 + (a + k_v k A_\theta)s + \alpha k A_\theta$ are complex conjugate, i.e., they can be written:

$$s^2 + (a + k_v k A_\theta)s + \alpha k A_\theta = (s + \sigma + j\omega)(s + \sigma - j\omega), \quad \sigma > 0, \quad \omega > 0.$$

According to rule 3, there are $n - m = 4$ root locus branches tending toward infinity on the plane s along four asymptotes whose angles are given as:

$$\frac{\pm 180^\circ}{4} = \pm 45^\circ,$$
$$\frac{\pm 180^\circ(3)}{4} = \pm 3(45^\circ) = \pm 135^\circ.$$

Hence, using these results in addition to rules 1,2 and 5, it is concluded that the possibilities depicted in Fig. 5.50 exist. According to rule 4, the point where these asymptotes intersect with the real axis is given as:

$$\sigma_a = \frac{-2\sigma + (b - c)}{4}.$$

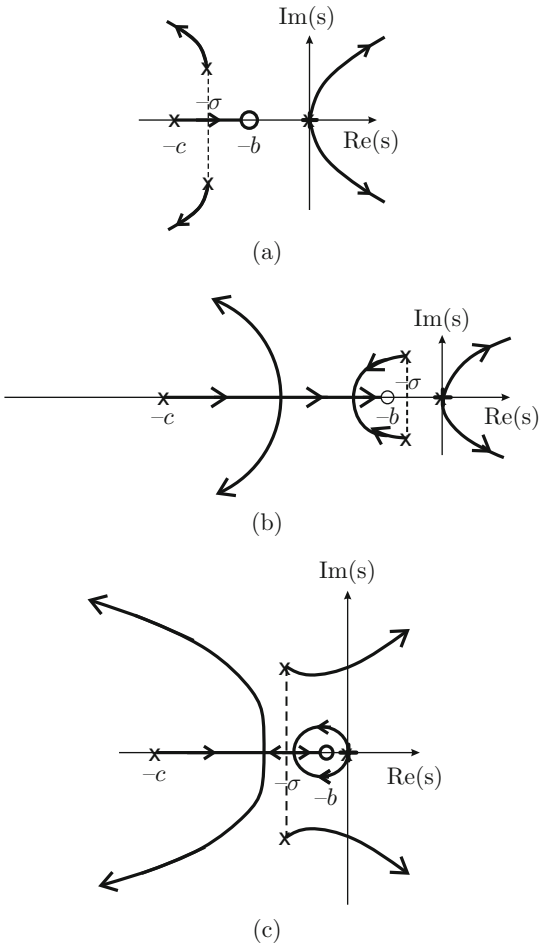

Fig. 5.47 Root locus possibilities for a ball and beam system

This means that the four branches are pulled to the left; hence, the closed-loop system becomes more stable, if:

- A greater $\sigma > 0$ is chosen, i.e., if the system:

$$\frac{\alpha k A_\theta}{s^2 + (a + k_v k A_\theta)s + \alpha k A_\theta}, \tag{5.52}$$

  is damped enough, which is accomplished using a large enough value for $k_v > 0$.
- $b > 0$ Approaches to zero and $c > 0$ are large, i.e., if $c > b$. Note that this is in agreement with rules 11 and 12.

Following the second item above, the root locus shown in Fig. 5.47b is obtained. Notice that both branches starting at the poles located at $s = 0$ always remain on

the right half-plane, i.e., the closed-loop system is unstable. The main reason for this behavior is that branches starting at the poles of the transfer function in (5.52) are pulled to the segment on the real axis between $s = -c$ and $s = -b$. This is because both open-loop complex conjugate poles are too close to the segment between $s = -c$ and $s = -b$. If these complex poles are placed far from such a segment, then the possibility exists for branches starting at $s = 0$ to be pulled to the segment between $s = -c$ and $s = -b$ to obtain the root locus diagram shown in Fig. 5.47c. This implies closed-loop stability for some of the small values of the loop gain. To achieve this, it is necessary to use large values for the coefficient $\alpha k A_\theta$ (because this increases the distance to the origin of the above-mentioned open-loop complex conjugate poles), i.e., using a large value for α.

According to the previous discussion, large values must be used for k_v and α. However, these values are limited in practice by the system noise content; hence, k_v and α must be obtained using experimental tests. In fact, noise is also an important reason not to select real poles for the transfer function in (5.52): real poles produce a very damped system that requires a large value for k_v. According to the experimental tests reported in Chap. 14 the following values were selected:

$$\alpha = 12, \quad k_v = 0.2.$$

Hence, the only values that remain to be determined are γ, c and b. Although these parameters can be determined such that the closed-loop poles are assigned at the desired locations (using the methodology presented in Sect. 5.2.6), in this case, it is preferred just to select them such that closed-loop stability is accomplished. To achieve this, we proceed as follows.

- b and c are proposed such that $c > b > 0$.
- MATLAB is employed to draw the root locus diagram.
- $\gamma > 0$ is chosen as that value placing all the closed-loop system poles on the left half-plane. This means that γ is the parameter used by the method to plot the root locus diagram.
- If such a $\gamma > 0$ does not exist, then we go back to the first step.

The root locus diagram shown in Fig. 5.48 is obtained following this procedure. It is observed that all the closed-loop poles, i.e., those indicated with a symbol "+," have a negative real part if:

$$\gamma = 1.2, \quad c = 20, \quad b = 2.5.$$

The simulation response of the closed-loop system when the reference is an unitary step is shown in Fig. 5.49. The graphical results in Figs. 5.48 and 5.49 were obtained by executing the following MATLAB code in an m-file:

```
Ax=5.375;
At=0.9167;
k=16.6035;
```

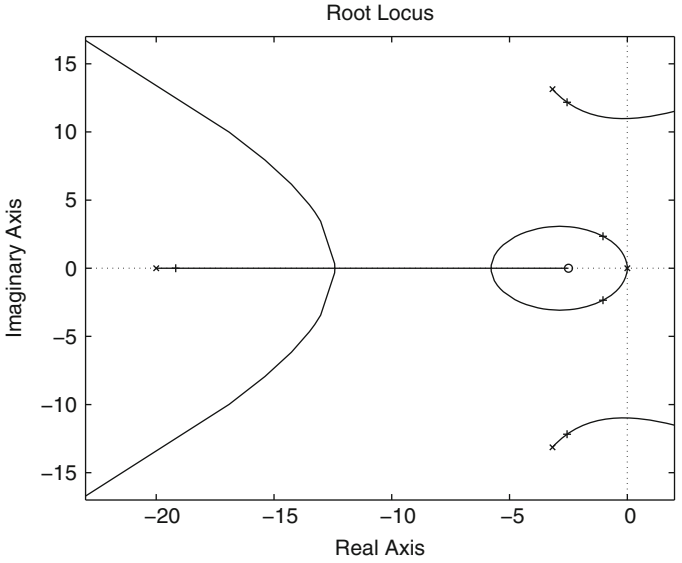

Fig. 5.48 Root locus diagram for the ball and beam system that has been designed

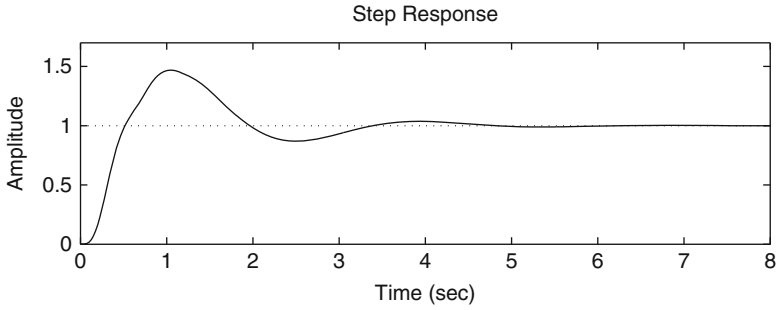

Fig. 5.49 The ball and beam closed-loop response

```
a=3.3132;
rho=5;
alpha=12;
kv=0.2;
c=20;
b=2.5;
gm=tf(k,[1 a 0]);
velFd=tf(kv*At*[1 0],1);
g1=feedback(gm,velFd,-1);
g2=feedback(alpha*g1,At,-1);
glead=tf([1 b],[1 c]);
```

```
gball=tf(rho,[1 0 0]);
gh=glead*g2*Ax*gball;
figure(1)
rlocus(gh);
axis([-23 2 -17 17])
gamma=rlocfind(gh)
M=feedback(gamma*gh,1,-1);
figure(2)
subplot(2,1,1)
step(M,8)
axis([0 8 0 1.7])
```

Finally, it is important to state that an additional step must be included:

- Once the values for γ, c and b are chosen, some experimental tests must be performed to verify that a good performance is obtained. If this is not the case, then we go back again to the first step in the procedure detailed above.

5.2.9 *Assigning the Desired Closed-Loop Poles for a Ball and Beam System*

Consider again the control problem in the previous section, but now using the following system parameters:

$$\rho = 4.8,\ a = 0.98,\ k = 10.729,\ k_v = 0.35,\ \alpha = 30,\ A_\theta = A_x = 1. \quad (5.53)$$

Suppose[3] that the transient response specifications are stated by requiring a rise time $t_r = 1$[s] and an overshoot $M_p = 25\%$. The use of this information and:

$$\zeta = \sqrt{\frac{\ln^2\left(\frac{Mp(\%)}{100}\right)}{\ln^2\left(\frac{Mp(\%)}{100}\right) + \pi^2}},$$

$$\omega_d = \frac{1}{t_r}\left[\pi - \arctan\left(\frac{\sqrt{1-\zeta^2}}{\zeta}\right)\right],$$

$$\omega_n = \frac{\omega_d}{\sqrt{1-\zeta^2}},$$

allows us to find that a complex closed-loop pole must be located at:

$$s = -\zeta\omega_n \pm j\omega_d = -0.8765 + j1.9864. \quad (5.54)$$

[3] At this point, the reader is advised to see Example 8.2 in Chap. 8.

According to the closed-loop block diagram shown in Fig. 5.46, the open-loop transfer function in (5.51) becomes:

$$G(s)H(s) = \gamma \frac{s+b}{s+c} \frac{1545}{s^4 + 4.735s^3 + 321.9s^2}. \tag{5.55}$$

Using these numerical values, it is found that the open-loop poles are located at:

$$s_1 = 0,\ s_2 = 0,\ s_6 = -2.3676 + j17.7838,\ s_5 = -2.3676 - j17.7838.$$

Consider Fig. 5.50a. Proceed as in Sect. 5.2.6. The angle and the magnitude conditions establish that:

$$\theta_3 - (\theta_1 + \theta_2 + \theta_4 + \theta_5 + \theta_6) = -180^\circ,$$
$$\frac{1545\gamma l_3}{l_1 l_2 l_4 l_5 l_6} = 1.$$

From these expressions, the following is found:

$$\theta_3 - \theta_4 = -180^\circ + (\theta_1 + \theta_2 + \theta_5 + \theta_6), \tag{5.56}$$
$$\gamma = \frac{l_1 l_2 l_4 l_5 l_6}{1545 l_3}. \tag{5.57}$$

Also notice that:

$$\theta_3 = 180^\circ - \arctan\left(\frac{1.9864}{0.8765 - b}\right), \tag{5.58}$$
$$\theta_4 = \arctan\left(\frac{1.9864}{c - 0.8765}\right),$$
$$\theta_1 = \theta_2 = 180^\circ - \arctan\left(\frac{1.9864}{0.8765}\right), \tag{5.59}$$
$$\theta_5 = \arctan\left(\frac{1.9864 + 17.7838}{2.3676 - 0.8765}\right), \tag{5.60}$$
$$\theta_6 = -\arctan\left(\frac{(17.7838 - 1.9864}{2.3676 - 0.8765}\right), \tag{5.61}$$
$$l_1 = l_2 = \sqrt{1.9864^2 + 0.8765^2},$$
$$l_3 = \sqrt{1.9864^2 + (0.8765 - b)^2},$$
$$l_4 = \sqrt{1.9864^2 + (c - 0.8765)^2},$$
$$l_5 = \sqrt{(17.7838 + 1.9864)^2 + (2.3676 - 0.8765)^2},$$
$$l_6 = \sqrt{(17.7838 - 1.9864)^2 + (2.3676 - 0.8765)^2}.$$

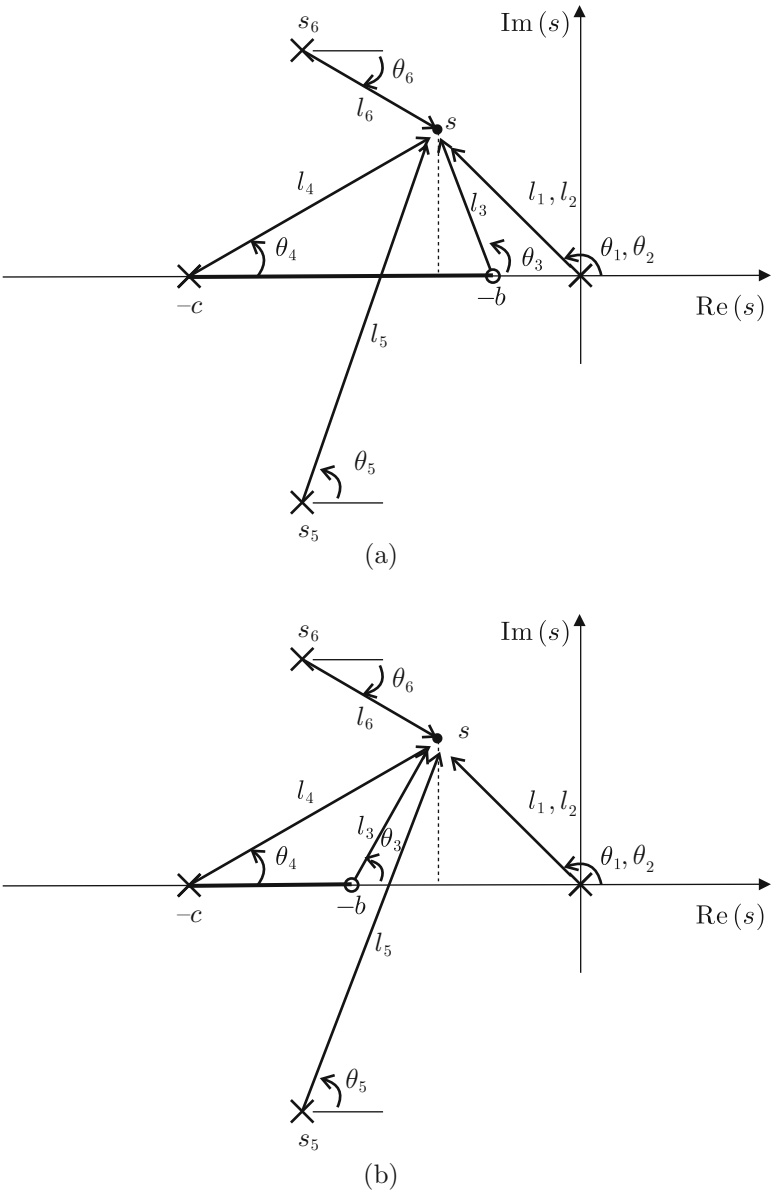

Fig. 5.50 Open-loop pole–zero contributions to the root locus diagram for a ball and beam system

From the second expression, the following is found:

$$c = \frac{1.9864}{\tan(\theta_4)} + 0.8765. \tag{5.62}$$

The following design procedure is proposed:

1. Compute $\theta_1, \theta_2, \theta_5, \theta_6$, using (5.59), (5.60), (5.61), and the difference $\theta_3 - \theta_4$ using (5.56).
2. Propose some b and compute θ_3 using (5.58). Using this and the value of the difference $\theta_3 - \theta_4$, compute θ_4.
3. Compute c and γ using (5.62) and (5.57) respectively.

Proposing $b = 0.7$, the above procedure yields $c = 2.8658$ and $\gamma = 1.3531$. The corresponding root locus diagram is depicted in Fig. 5.51 where the closed-loop poles are marked using the symbol "+". Notice that the desired closed-loop pole at $-0.8765 + j1.9864$ has been successfully assigned. In Fig. 5.52, we present the time response of the closed-loop system (continuous) when a unit step reference is applied. We also present, with a dashed line, the time response of the system:

$$M(s) = \frac{\omega_n^2}{s^2 + 2\zeta\omega_n s + \omega_n^2}, \tag{5.63}$$

where the values for ω_n and ζ ensure that the poles are identical to those defined in (5.54), i.e., the dashed line represents the desired response. An important difference between these time responses is observed. In particular, overshoot is almost twice its desired value. This difference may be explained by the fact that the closed-loop transfer function of the system in Fig. 5.46 has a zero[4] at $s = -b$. This feature deviates the time response from its desired behavior represented by the dashed line, i.e., the second-order system without any zero defined in (5.63).

Thus, to solve this problem it is proposed to use the block diagram in Fig. 5.53. Notice that the only difference with respect to the block diagram in Fig. 5.46 is that the lead-compensator $\gamma\frac{s+b}{s+c}$ is now placed in the feedback path. The reason for this is that the resulting closed-loop transfer function now has no zero.[5] Notice that the root locus diagram in this case is identical to that in Fig. 5.51 as the open-loop transfer function in this case $G(s)H(s)$ is identical to that in (5.55) because $b = 0.7$, $c = 2.8658$, $\gamma = 1.3531$ again. Recall that the zero at $s = -b$ is no longer closed-loop zero. The closed-loop time response for the block diagram in Fig. 5.53 is presented in Fig. 5.54 with a continuous line, whereas the desired response is represented by the dashed line. Notice that, again, an significant difference exists between the achieved response and the desired response. Analyzing the root locus diagram in Fig. 5.51, it is observed that a closed-loop real pole at ≈ -0.95 is very close to the poles at $-0.8765 \pm j1.9864$, which determine the transient response. Hence, the effects of this real pole are not negligible, and they are important in the transient response: the closed-loop system behaves as a third-order system instead of a second-order system. This fact explains the lag observed in the response achieved in Fig. 5.54.

[4] It is left as an exercise for the reader to verify this fact.

[5] Again, it is left as an exercise for the reader to verify this fact.

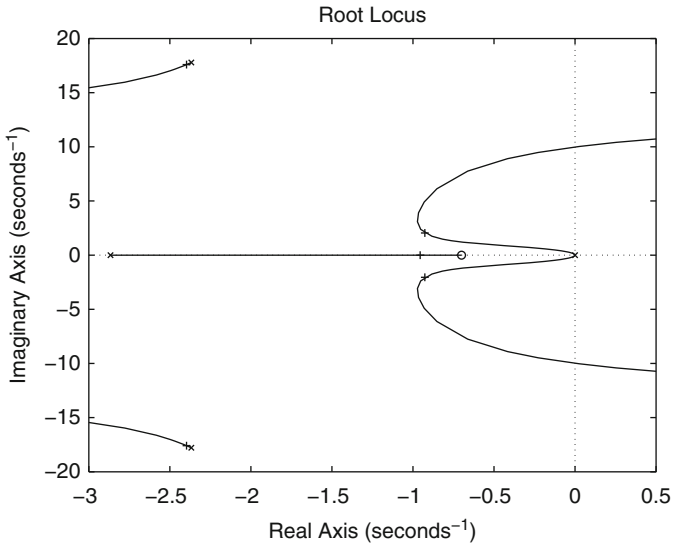

Fig. 5.51 Root locus diagram for the ball and beam system when using the block diagram in Fig. 5.46 and the controller gains $b = 0.7$, $c = 2.8658$, $\gamma = 1.3531$

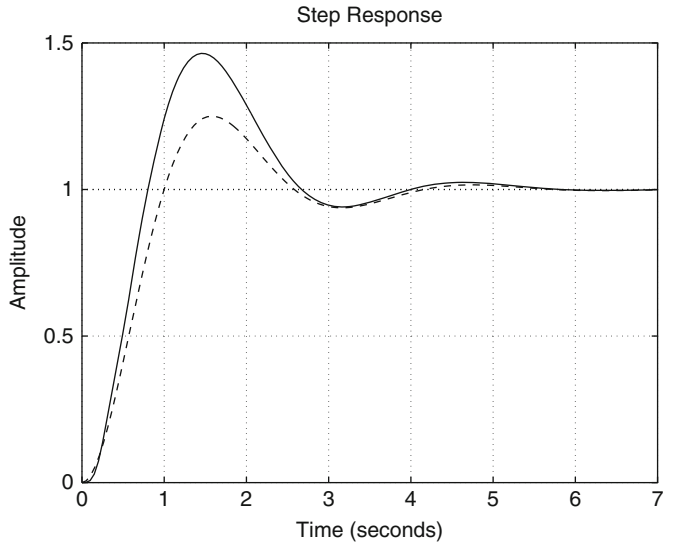

Fig. 5.52 Closed-loop time response of the ball and beam system when using the block diagram in Fig. 5.46 and the controller gains $b = 0.7$, $c = 2.8658$, $\gamma = 1.3531$ (continuous). Dashed: desired response

Hence, a remedy for this problem is to place this real pole further to the left. This may be accomplished by placing the zero at $s = -b$ further to the left as depicted

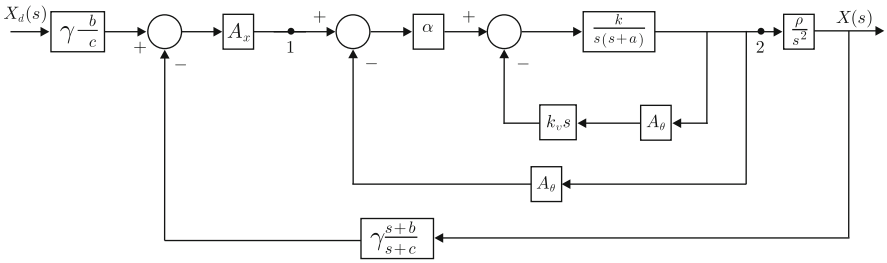

Fig. 5.53 Use of the lead compensator in the feedback path. The factor $\gamma\frac{b}{c}$ on the left is included to ensure that $\lim_{t\to\infty} x(t) = x_d$

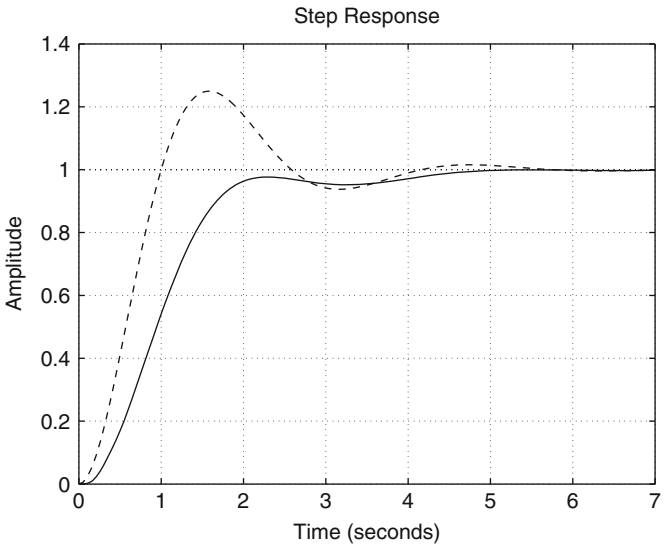

Fig. 5.54 Closed-loop time response of the ball and beam system when using the block diagram in Fig. 5.53 and the controller gains $b = 0.7$, $c = 2.8658$, $\gamma = 1.3531$ (continuous). Dashed: desired response

in Fig. 5.50b. Notice that in this case:

$$\theta_3 = \arctan\left(\frac{1.9864}{b - 0.8765}\right). \tag{5.64}$$

Thus, the design procedure proposed above is still valid, only requiring use of (5.64) instead of (5.58). Hence, proposing $b = 1.4$, the following is found: $c = 5.1138$ and $\gamma = 2.1868$. The root locus diagram for this case is shown in Fig. 5.55 where the closed-loop poles are marked with the symbol "+." It can be seen that the real pole is now placed at about -3.5, far enough from the poles in (5.54). Moreover, the time response achieved in this case (continuous) is shown in Fig. 5.56 and compared with

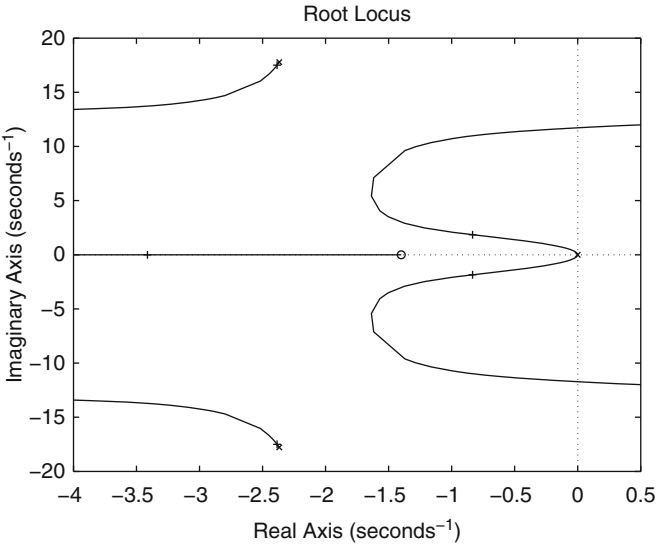

Fig. 5.55 Root locus for the ball and beam system according to the block diagram in Fig. 5.53 and controller gains $b = 1.4$, $c = 5.1138$, $\gamma = 2.1868$

the desired response (dashed). We realize that both responses are very similar in this case, which corroborates the correctness of the design. This controller is tested experimentally in Chap. 14.

Finally, to further improve the transient response, in Figs. 5.57 and 5.58, the root locus diagram and the time response respectively are shown when using the controller gains $b = 2$, $c = 11.7121$ and $\gamma = 4.6336$. Note that the real pole is now placed at about -10.5, i.e., it is far from the poles in (5.54). This results in a very small effect of this pole on the transient response, which, as shown in Fig. 5.58, is now very close to the desired response.

Except for Figs. 5.50 and 5.53, all the figures in this section have been drawn using the following MATLAB code in an m-file:

```
clc
clear
rho=4.8;
a=0.98;
k=10.729;
kv=0.35;
alpha=30;
Ao=1;
Ax=1;
Gdcm=tf(k,[1 a 0]);
Gfvel=tf(kv*Ao*[1 0],1);
Gfdbk1=feedback(Gdcm,Gfvel,-1);
```

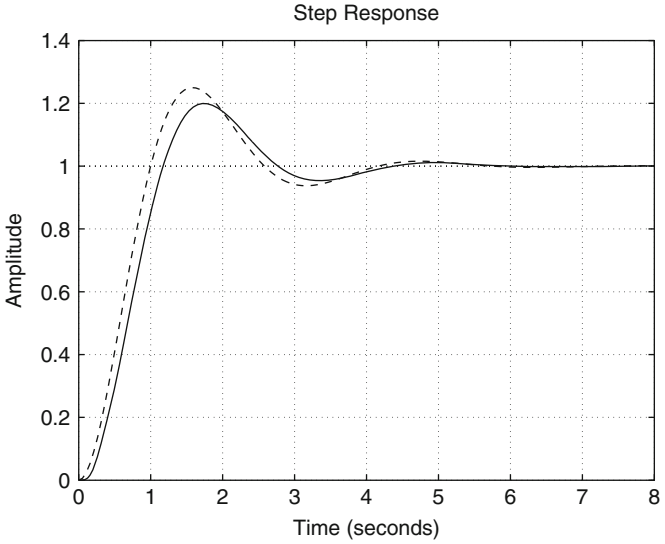

Fig. 5.56 Closed-loop time response of the ball and beam system according to the block diagram in Fig. 5.53 and controller gains $b = 1.4$, $c = 5.1138$, $\gamma = 2.1868$ (continuous). Dashed: desired response

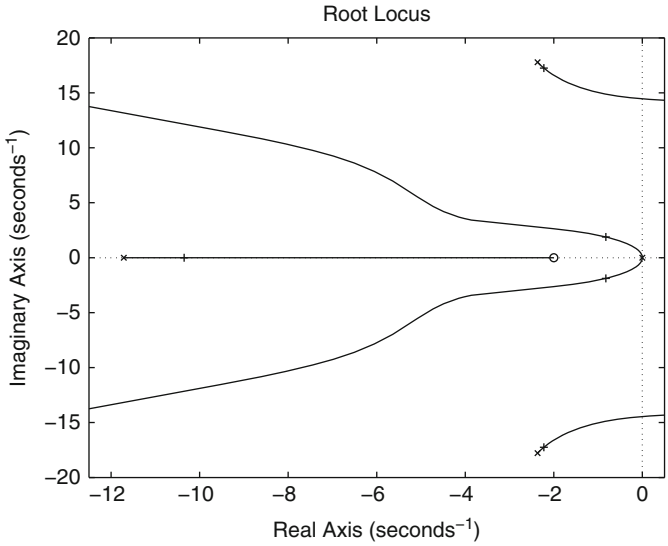

Fig. 5.57 Root locus diagram for the ball and beam system when using the block diagram in Fig. 5.53 and the controller gains $b = 2$, $c = 11.7121$ and $\gamma = 4.6336$

```
G2=alpha*Gfdbk1;
Gfdbk2=feedback(G2,Ao,-1);
```

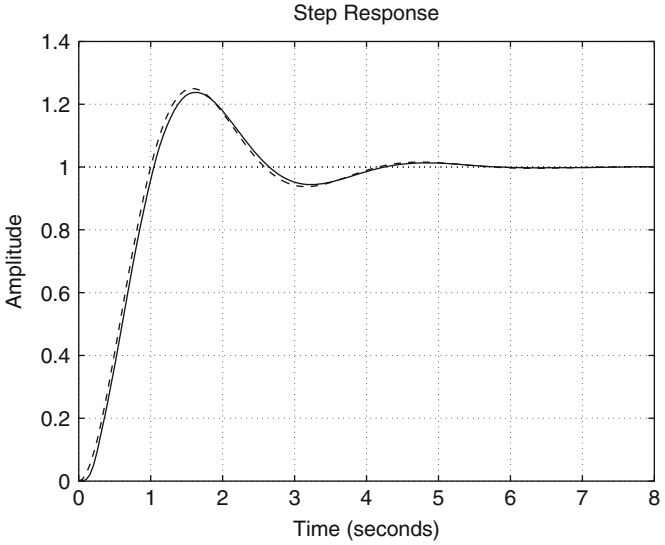

Fig. 5.58 Closed-loop time response of the ball and beam system when using the block diagram in Fig. 5.53 and the controller gains $b = 2$, $c = 11.7121$ and $\gamma = 4.6336$ (continuous). Dashed: desired response

```
Gball=tf(rho,[1 0 0]);
GH=Ax*Gfdbk2*Gball
pole(GH)
figure(1)
rlocus(GH)
axis([-5 2 -30 30])
tr=1; %s
Mp=25;%
z=sqrt(log(Mp/100)^2/(pi^2+log(Mp/100)^2));
wn=1/(tr*sqrt(1-z^2))*(pi-atan(sqrt(1-z^2)/z));
wd=wn*sqrt(1-z^2);
Res=-z*wn % -0.8765
Ims=wd % j 1.9864
th1=pi-atan(Ims/(-Res));
th5=atan((Ims+17.7838)/(2.3676+Res));
th6=-atan((17.7838-Ims)/(2.7636+Res));
th3menosth4=-pi+(2*th1+th5+th6);
b=2
%b=1.4
%b=0.7
%th3=pi-atan(Ims/(-Res-b));
th3=atan(Ims/(b+Res));
```

```
th4=-th3menosth4+th3;
c=Ims/tan(th4)-Res
l1=sqrt(Ims^2+Res^2);
l3=sqrt(Ims^2+(-Res-b)^2);
l4=sqrt(Ims^2+(c+Res)^2);
l5=sqrt((17.7838-Ims)^2+(2.3676+Res)^2);
l6=sqrt((17.7838+Ims)^2+(2.3676+Res)^2);
gamma=l1^2*l4*l5*l6/(l3*rho*alpha*k*Ax)
ctrl=tf(gamma*[1 b],[1 c]);
GHcomp=GH*ctrl;
gg=0:0.01:1;
figure(2)
rlocus(GHcomp) %,gg)
axis([-12.5 0.5 -20 20])
rlocfind(GHcomp)
M=feedback(GH,ctrl,-1);
M1=tf(wn^2,[1 2*z*wn wn^2])
figure(3)
step(M*0.7913,'b-',M1,'r--')
%step(M*0.5987,'b-',M1,'r--')
%step(M*0.3305,'b-',M1,'r--')
grid on
```

5.3 Case Study: Additional Notes on the PID Control of Position for a Permanent Magnet Brushed DC Motor

The PID control for position regulation in a DC motor is studied in Sect. 5.2.5. There, it was found that the motor position relates to the desired position and an external torque disturbance through two transfer functions, which, however, have the same characteristic polynomial:

$$s^3 + (a + k_d k)s^2 + k_p k s + k_i k. \tag{5.65}$$

It was also found that the following closed-loop poles p_1, p_2, p_3 can be assigned:

$$p_1 = \sigma_1 + j\omega_1, \quad p_2 = \sigma_2 - j\omega_1, \quad p_3 < 0, \quad \sigma_1 < 0, \quad \sigma_2 < 0, \quad \omega_1 \geq 0.$$

Notice that $\sigma_1 = \sigma_2$ if $\omega_1 > 0$, i.e., when a pair of complex conjugate poles exists, but $\sigma_1 \neq \sigma_2$ is possible when $\omega_1 = 0$. Then, controller gains must be selected according to:

$$k_d = \frac{-(\sigma_1 + \sigma_2 + p_3) - a}{k} > 0, \tag{5.66}$$

$$k_p = \frac{\sigma_1\sigma_2 + \omega_1^2 + p_3\sigma_1 + \sigma_2 p_3}{k} > 0, \tag{5.67}$$

$$k_i = \frac{-p_3(\sigma_1\sigma_2 + \omega_1^2)}{k} > 0. \tag{5.68}$$

On the other hand, in Example 4.12, Chap. 4, it was found that all of the roots of the following polynomial:

$$s^3 + as^2 + bs + c,$$

have a negative real part if and only if:

$$a > 0, \quad b > \frac{c}{a} > 0 \quad c > 0,$$

Applying these conditions to the characteristic polynomial in (5.65), yields:

$$a + k_d k > 0, \quad k_p k > \frac{k_i k}{a + k_d k}, \quad k_i k > 0. \tag{5.69}$$

Using the expressions in (5.66), (5.67), (5.68), (5.69), Fig. 5.59, the results in Sect. 3.3, and Example 3.9, the effects of the PID controller gains on the closed-loop system response can be studied.

- $k_p > 0$ and $k_d > 0$ are small, whereas $k_i > 0$ is large.
  - Suppose that p_1 and p_2 are complex conjugate. Then, $\omega_n^2 = \sigma_1\sigma_2 + \omega_1^2$ in Fig. 5.59. According to (5.68), the product $-p_3\omega_n^2$ is large, which implies a faster response because a real pole produces faster responses as p_3 moves to the left and a second-order system is faster as ω_n is larger. Note that k_i can be kept constant and, according to (5.67), $k_p > 0$ can be rendered small if both σ_1 and σ_2 approach zero, i.e., if $\theta > 0$ in Fig. 5.59 approaches zero and, hence, damping approaches zero (without affecting ω_n nor $-p_3$). According to (5.66), this also renders $k_d > 0$ small. Also notice that this is in agreement with the second inequality in (5.69), i.e., $k_p k > \frac{k_i k}{a + k_d k}$. If $k_i > 0$ is large and $k_p > 0$, $k_d > 0$ are small, then this condition tends not to be valid, i.e., the closed-loop system approaches instability and becomes more oscillatory.
  - Suppose that p_1 and p_2 are real and different, i.e., $\omega_1 = 0$. Thus, a more damped and, hence, slower response is obtained. According to (5.68), this results in a smaller $k_i > 0$. However, according to (5.66), (5.67), $k_p > 0$, and $k_d > 0$ can be rendered larger because $|\sigma_1|$ may become larger despite σ_2 approaching zero. Thus, from the second inequality in (5.69), it is concluded too that a more damped response is obtained.
    Notice that an increment in $k_d > 0$ has a greater effect on the increment of $|\sigma_1|$ than the effect that an increment in $k_p > 0$ has on the increment of $|\sigma_1|$ because this real part is affected by p_3 in (5.67), which is assumed to be large.

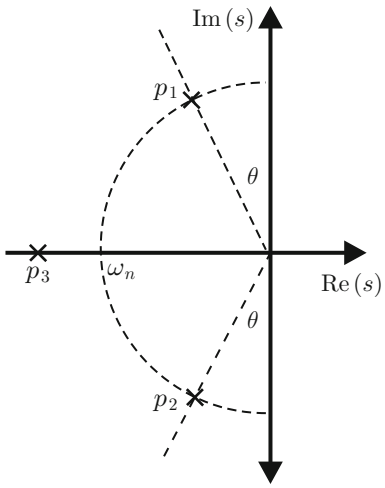

Fig. 5.59 Closed-loop pole location for PID position control in a DC motor

Thus, it is concluded that k_d has a greater effect on the damping than k_p, i.e., the slower response predicted above is more affected by k_d.

- $k_i > 0$ is small and $k_p > 0$ is large.
  This may be possible if p_3 is close to zero and p_1 and p_2, are complex conjugate. Thus, according to (5.67) and (5.66), $k_p > 0$ can be large and $k_d > 0$ small if $\omega_n^2 = \sigma_1\sigma_2 + \omega_1^2$ is large and σ_1 and σ_2, are close to zero. This means that the damping is small because $\theta > 0$ in Fig. 5.59 is close to zero. Thus, a more oscillatory but faster closed-loop system response is obtained.
  However, $|\sigma_1|$ and $|\sigma_2|$ may be rendered larger, i.e., to increase $k_d > 0$, without affecting ω_n if $\theta > 0$ in Fig. 5.59 is increased. Thus, a more damped but slower system response is obtained. Notice that $k_p > 0$ is less affected by the changes in $|\sigma_1|$ and $|\sigma_2|$ because they are affected by p_3 in (5.67), which is assumed to be close to zero.

According to the discussion above the following is concluded regarding the effects that the PID control gains have when used for position regulation in a DC motor:

- Larger positive values for the integral gain, k_i, result in a faster response that becomes more oscillatory.
- Large positive values of the proportional gain, k_p, result in either *a*) a slightly more damped response if $k_i > 0$ is large, or *b*) a more oscillatory response if $k_i > 0$ is small. In both cases, a fast response is expected.
- Larger positive values of the derivative gain, k_d, produce a more damped and slower response.

It is convenient to say that the transfer function between the position and its desired value ($G_1(s)$ in (5.26)) has two zeros whose effect on the transient response is not completely clear. Hence, it is possible that sometimes, some variations appear

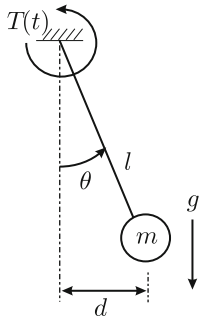

Fig. 5.60 Simple pendulum used as a load for a DC motor

regarding the effects that have just been described for the gains of the PID controller. Furthermore, the fact that the external disturbance is present because the desired position is commanded in some mechanisms may favor these variations.

To illustrate the ideas above, some experimental results that were obtained when controlling the position of a DC motor are presented in the following. The experimental prototype is the same as that described in Chap. 11 with a simple modification (that is not present in that chapter): the pendulum shown in Fig. 5.60 is fixed to the motor shaft. Hence, by means of the gravity effect g, a torque disturbance is introduced that tries to deviate the motor position from its desired value. In Fig. 5.60, $T(t)$ represents the torque generated by the motor and θ is the controlled variable. The pendulum parameters l and m are not measured to show that a PID controller can be tuned without any necessity of knowing the plant, if the effects of the controller gains (listed above) are well understood.

The corresponding experimental results are presented in Figs. 5.61 and 5.62. The desired position is set to $\theta_d = \pi/2$[rad] as this is where the torque disturbance due to gravity has its greatest effect. A vertical line at $t = 0.13$[s] and a horizontal line at $\theta = 1.8$[rad] are also shown to indicate the desired rise time and overshoot. Only one parameter is adjusted each time to clearly appreciate its effect. Curves drawn in Fig. 5.61 correspond to the following PID controller gains:

1. Upper figure:
   - Continuous: $k_p = 0.5, k_i = 0, k_d = 0$
   - Dash–dot: $k_p = 1, k_i = 0, k_d = 0$
   - Dotted: $k_p = 1, k_i = 0, k_d = 0.05$
2. Bottom figure:
   - Continuous: $k_p = 1, k_i = 2, k_d = 0.05$
   - Dash–dot: $k_p = 1, k_i = 5, k_d = 0.05$
   - Dotted: $k_p = 2, k_i = 5, k_d = 0.05$
   - Dashed: $k_p = 2, k_i = 5, k_d = 0.1$

As the closed-loop system is third-order when a PID controller is used and the motor parameters are not known, it is difficult to know the controller gains that ensure

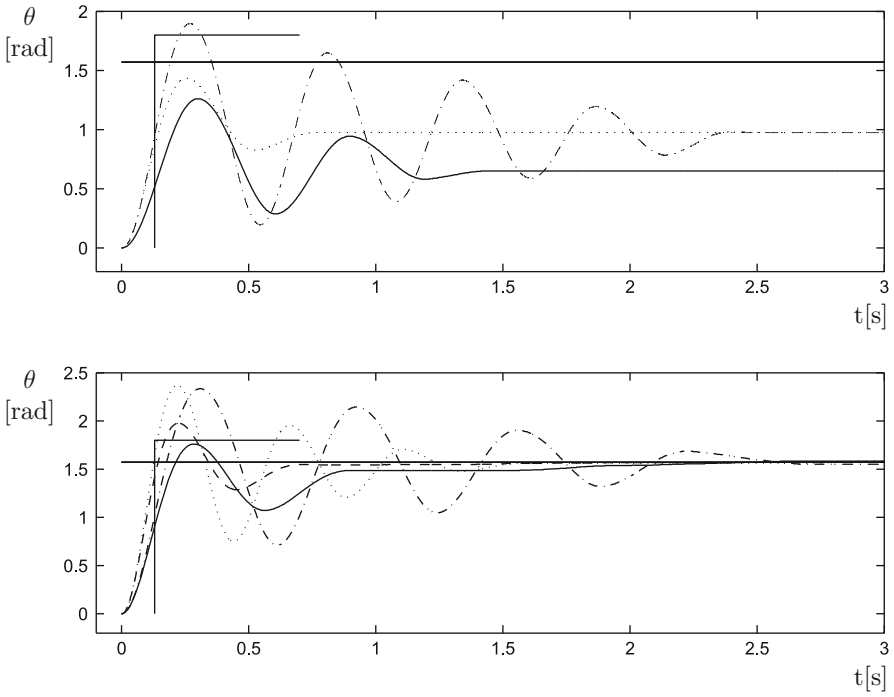

Fig. 5.61 The PID control of position for a DC motor with a pendulum as a load. Experimental results

stability. Thus, the best that can be done is to begin with a PD controller (assigning $k_i = 0$), which produces a second-order closed-loop system that is stable for any positive k_p with $k_d = 0$ (because any real mechanism possesses friction). Later, according to the transient response obtained and to the tuning rules listed above, the gains k_i and k_d are introduced such that stable responses are accomplished. It is for this reason that, in the upper part of Fig. 5.61 a PD controller is employed. Note that a steady-state error that is different from zero is obtained because of the torque disturbance introduced by gravity (recall that $k_i = 0$). The aim in this part of the experiment is to allow the system response time to approach its desired value ensuring stable behavior. Thus, the proportional gain is first increased to $k_p = 1$ and then the derivative gain is increased to $k_d = 0.05$. Then, an integral term can be introduced, which, although producing a zero steady-state error, increases the oscillations in the system response. This is shown at the bottom part of Fig. 5.61. Again, the idea is to allow the response time to approach its desired value. This is accomplished first by increasing the integral gain to $k_i = 5$. As this also increases the oscillation, $k_p = 2$ is employed to render the system response faster without appreciably increasing the oscillation. Finally, $k_d = 0.1$ is used to produce a well damped response. Notice that the increment on k_d increases the rise time a little.

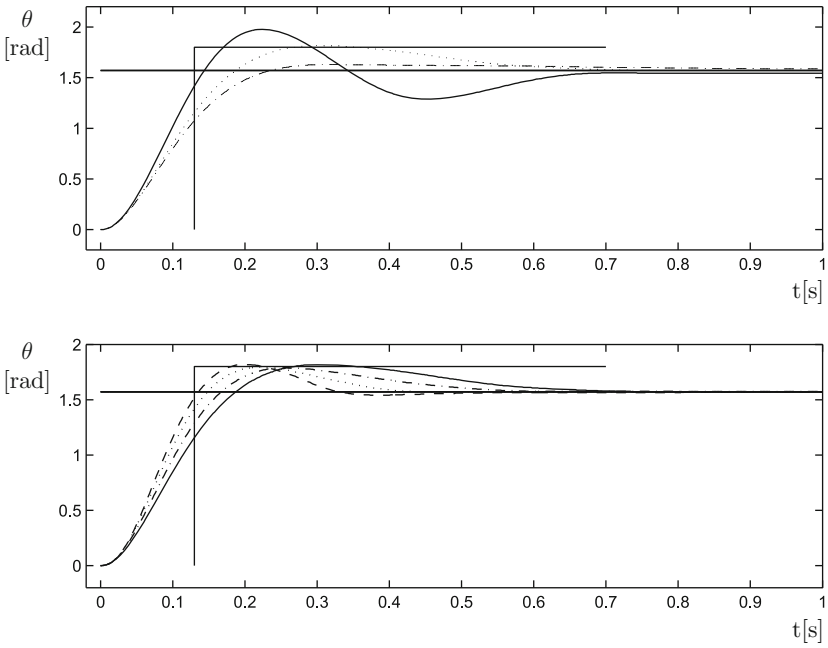

Fig. 5.62 The PID control of position for a DC motor with a pendulum as a load. Experimental results

Curves drawn in Fig. 5.62 correspond to the following PID controller gains:

1. Upper figure:
   - Continuous: $k_p = 2, k_i = 5, k_d = 0.1$
   - Dash–dot: $k_p = 2, k_i = 5, k_d = 0.2$
   - Dotted: $k_p = 2, k_i = 8, k_d = 0.2$
2. Bottom figure:
   - Continuous: $k_p = 2, k_i = 8, k_d = 0.2$
   - Dash–dot: $k_p = 2.5, k_i = 8, k_d = 0.2$
   - Dotted: $k_p = 3, k_i = 8, k_d = 0.2$
   - Dashed: $k_p = 3.5, k_i = 8, k_d = 0.2$

In the upper part of Fig. 5.62, it is observed that the response is even more damped and slower when the derivative gain is increased from $k_d = 0.1$ to $k_d = 0.2$. Because, at this moment, the response is slow and overshoot is small, $k_i = 8$ is employed to render the response faster and with a larger overshoot that is equal to the desired overshoot. To render the system faster, without appreciably affecting overshoot, the proportional gain is increased to $k_p = 3.5$ in the lower part of Fig. 5.62. This allows the desired rise time and overshoot to be accomplished.

It is important to stress the following. When connecting the pendulum to the motor shaft, the control system becomes nonlinear. This means that the control system behavior is not correctly predicted by the analysis presented above at certain operation regions. For instance, if the desired position is close to $\theta_d = \pm\pi$, a simple PD controller may be unstable if the proportional gain (positive) is not greater than a certain lower threshold. This result is obtained using a PD controller for the case when $x_1^* = \pm\pi$, $x_2^* = 0$ in Example 7.5 studied in Chap. 7 by finding the poles for such a linear approximation. The reader may also see the works reported in [2, 4], ch. 8, [3], ch. 7. This situation is worse for the case of a PID controller, but the problem does not appear if the desired position value is kept far from $\theta_d = \pm\pi$, as in the results presented in this section.

Finally, notice that the selection of the PID controller gains has been performed without requiring knowledge of the numerical value of any motor or pendulum parameter. However, the minimal knowledge that must be available is to verify that the motor can produce the required torque to perform the task. This must include the required torque to compensate for the gravity effect plus some additional torque to achieve the desired rise time.

5.4 Summary

The most general method of controller design using the time response approach is the root locus method. This means that the plants that can be controlled are of arbitrary order with any number of zeros as long as they are less than the number of poles. This method provides the necessary tools to determine, in a graphical way, the location of the closed-loop poles from the location of the open-loop poles and zeros. Some of the open-loop poles and zeros are due to the controller and the idea of the method is to select the location of the controller poles and zeros such that the desired closed-loop poles are assigned. The desired closed-loop poles are chosen from the knowledge of how they affect the corresponding transient response. The study presented in Chap. 3 is important for this. On the other hand, the controller structure is chosen from the knowledge of how the open-loop poles and zeros affect the closed-loop system steady- state response. The study presented in Chap. 4 is very important for this.

Although the root locus has been presented as a controller design method, it is also a powerful tool for control systems analysis. This means that it can be used to determine: (i) The relative stability of a control system, (ii) How the control system response changes as one of its parameters changes, (iii) What has to be done to modify the control system properties, etc. The use of the root locus method in these applications depends, to a large extent, on a good understanding of the method and the material presented in Chaps. 3 and 4.

5.5 Review Questions

1. When would you use each one of the following controllers?
   - Proportional.
   - Proportional–derivative.
   - Proportional–integral.
   - Proportional–integral–derivative.
2. Why do you think it is not advised to use the following controllers: (i) Derivative (alone), (ii) Integral (alone), and (iii) Derivative–integral (alone), i.e., without including a proportional part? Explain.
3. How do the requirements of the steady-state error determine the poles and/or zeros of a controller, i.e., the controller structure?
4. What is the main component that a controller must possess to improve the closed-loop system stability? What is the effect of this on the shape of the root locus diagram?
5. What is the main component that a controller must possess to improve the steady-state error? What is the effect of this on the shape of the root locus diagram?
6. Why does the root locus begin at the open-loop poles and end at the open-loop zeros? What do the words "begin" and "end" mean?
7. If the open-loop transfer function has no zeros, where does the root locus end?
8. It is often said that closed-loop system instability appears as the loop gain increases. However, this is not always true, because this depends on the properties of the plant to be controlled. Review the examples presented in this chapter and give an example of a plant requiring the loop gain to be large enough to render the closed-loop system stable.
9. What is a lead compensator and what is its main advantage?
10. Read Appendix F and Sect. 9.2 in Chap. 9. Use this information to explain how to practically implement a PID controller and a lead compensator using both software and analog electronics.

5.6 Exercises

1. Consider the control system in Fig. 5.63 where:

   $$k = 35.2671, \quad a = 3.5201, \quad c = 10.3672, \quad \gamma = 2.0465, \qquad d = 3.8935.$$

   Verify that two closed-loop complex conjugate poles exist at $s = -4.8935 \pm j6.6766$ when $k_i = 0$ and $k_p = 1$. Use MATLAB to draw the root locus for the following values of k_i:

   $$k_i = 0.001,\ 0.01,\ 0.1,\ 1,\ 10,$$

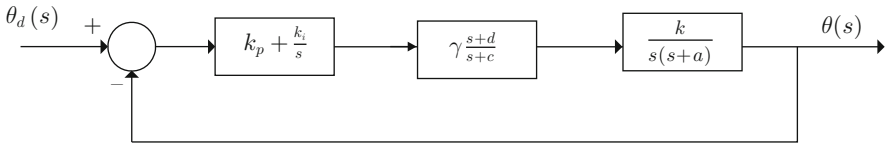

Fig. 5.63 A cascade connection of the PI control and lead compensator

Use k_p as the parameter the method varies from 0 to $+\infty$ to draw the root locus diagram. Select $k_p = 1$ and observe what happens with the closed-loop poles corresponding to $s = -4.8935 \pm j6.6766$. Perform simulations for each case when the reference is a unit step. Compare the obtained response as k_i grows with the response obtained when $k_p = 1$ and $k_i = 0$. Draw the corresponding root loci using the method presented in this chapter and explain what happens.

2. Consider the following plant:

$$Y(s) = H_1(s)U(s), \quad H_1(s) = \frac{k}{s(s+a)}, \quad k = 35.2671, \quad a = 3.5201.$$

a) Employ (3.71) in Chap. 3 to find the values for k_p and k_v such that the following transient response specifications are satisfied:

$$t_r = 0.33[\text{s}], \quad M_p(\%) = 10,$$

when y_d is a unit step and the following controller is used: $u(t) = k_p(y_d - y) - k_v\dot{y}$.

b) Assume that the input is given as:

$$u(t) = k_p(y_d - y) + k_d\frac{d(y_d - y)}{dt}, \quad \text{PD control.}$$

Obtain the closed-loop transfer function and use (3.71) in Chap. 3 to determine k_p and k_d such that the closed-loop poles are located at some points determining the following closed-loop transient response specifications:

$$t_r = 0.33[\text{s}], \quad M_p(\%) = 10.$$

Perform simulations corresponding to each one of the above items and compare the obtained responses. What is the reason for the differences between these responses? May zeros of a transfer function affect the transient response? Can these differences be explained using the root locus?

3. Consider a closed-loop system such as that shown in Fig. 5.1 with $H(s) = 1$ and $G(s) = \frac{1}{s^3+s^2+s+1}$.

- Using the rules presented in Sect. 5.1.1, draw the root locus diagram when using a proportional controller. Use Routh's criterion to determine the values of the proportional gain ensuring closed-loop stability.
- To stabilize the closed-loop system and to achieve a zero steady-state error when the reference is a step, design a PID controller proceeding as follows. (i) Propose $k_d s^2 + k_p s + k_i = k_d(s - z_1)(s - z_2)$, with $z_1 = -0.5 + 1.3j$, $z_2 = -0.5 - 1.3j$. Using the rules presented in Sect. 5.1.1, draw the root locus diagram to verify that no positive value exists for the derivative gain rendering the closed-loop system stable. (ii) Propose $k_d s^2 + k_p s + k_i = k_d(s - z_1)(s - z_2)$, with $z_1 = -0.25 + 1.3j$, $z_2 = -0.25 - 1.3j$. Using the rules presented in Sect. 5.1.1, draw the root locus diagram to verify that a range of positive values exists for the derivative gain k_d, rendering the closed-loop system stable. Use Routh's criterion to find the range of values for k_d, rendering the closed-loop system stable.
- How should the zeros of a PID controller be selected to improve the stability of the closed-loop system?

4. Verify that the transfer function of the circuit shown in Fig. 5.64 is:

$$\frac{V_o(s)}{V_i(s)} = \frac{s+a}{s+b}, \quad a = \frac{1}{R_1 C}, \quad b = \frac{1}{R_1 C} + \frac{1}{R_2 C}.$$

As $b > a$, this electric network can be used as a lead compensator.

5. Consider the following plant:

$$G(s) = \frac{4(s+0.2)}{(s+0.5)(s^2 - 0.2s + 0.3)}.$$

Use the root locus method to design a controller, ensuring closed-loop stability and a zero steady-state error when the reference is a step. It is suggested that the location of the poles and the zeros of the controller are proposed and then the open-loop gain is selected such that all the closed-loop poles have a negative real part.

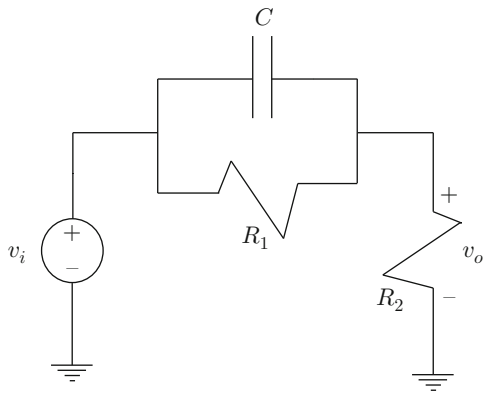

Fig. 5.64 A lead compensator

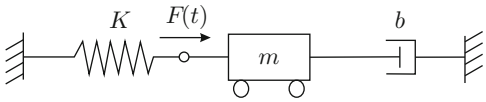

Fig. 5.65 A mass-spring-damper system

6. Consider the PD control of the position in Fig. 5.2.2. Prove that the value of the derivative gain k_d does not have any effect on the steady-state error when the reference is a step.
7. Consider the PID control of the position studied in Sect. 5.2.5. Prove that the values of the proportional k_p and the derivative k_d gains do not have any effect on the steady-state error, despite a constant disturbance being present if the reference is also constant.
   Assume that the integral part of the controller is not present, i.e., that $k_i = 0$. Prove that the value of the derivative gain k_d does not have any effect on the steady-state error.
8. Consider the mass-spring-damper system shown in Fig. 5.65, which has been modeled in Example 2.1, Chap. 2. In Example 3.18, Chap. 3, it is explained why a steady-state error that is different from zero exists when a proportional controller is employed and the desired position x_d is a constant that is different from zero. Recall that the force $F(t)$ applied to the mass is the control signal.
   Now suppose that a PID controller is used to regulate the position. Find the steady-state error when the desired position x_d is a constant that is different from zero. Use your everyday experience to explain your response, i.e., try to explain what happens with the force applied to the mass and the effect of the spring.
9. Consider the simple pendulum studied in Example 2.6, Chap. 2, which is shown in Fig. 5.66. Notice that the gravity exerts a torque that is different from zero on the pendulum if the angular position θ is different from zero. Suppose that it is desired to take the pendulum position θ to the constant value $\theta_d = 90°$. Note that torque $T(t)$ is the input for the pendulum. Using the experience in the previous exercise, state which controller you would employ to compute $T(t)$ such that θ reaches θ_d. Explain why. This problem is contrived to be solved without using a mathematical model; you merely need to understand the problem. In fact, the mathematical model is in this case nonlinear; hence, it cannot be analyzed using the control techniques studied in this book so far.
10. Consider an arbitrary plant $G(s)$ in cascade with the following controllers:

$$G_c(s) = \frac{s+a}{s+b}, \quad 0 < a < b,$$

$$G_d(s) = \frac{s+c}{s+d}, \quad c > d > 0.$$

$G_c(s)$ is known as a lead compensator, whereas $G_d(s)$ is known as a *lag compensator*.

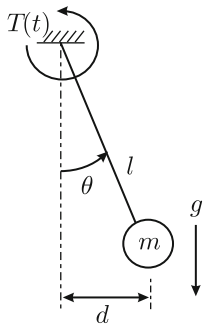

Fig. 5.66 A simple pendulum

- What is the effect of each one of these compensators on the steady-state error when the reference is a step?
- What is the effect of each one of these compensators on the closed-loop stability?
- Which compensator is related to PI control and which to PD control? Explain why.
- How would you employ these compensators to construct a controller with similar properties to those of PID control? Explain.

11. In a ship, it is common to have a unique compass to indicate the course. However, it is important to know this information at several places in the ship. Hence, it is common to transmit this information to exhibit it using a needle instrument. The angular position of the needle is actuated using a DC motor by using the information provided by the compass as the desired position. Design a closed-loop control system such that the needle position tracks the orientation provided by the compass according to the following specifications:

    - When a step change of 8° appears in the orientation provided by the compass, the system error decreases and remains at less than 1° in 0.3 s or less and overshoot is less than or equal to 25%.
    - When the orientation provided by the compass changes as a ramp of 5° per second, the steady-state error must be 0.3° or less.
    - There are no external disturbances.

    Under which ship operating conditions may these situations appear? The transfer function between the voltage applied to the motor and the needle position in degrees is:

$$G(s) = \frac{45.84 \times 10^{-5}}{s(4.4 \times 10^{-9}s^2 + 308.5 \times 10^{-9}s + 3.3 \times 10^{-6})}.$$

    Hint.
    (*i*) On the basis of the specifications indicated, choose a controller to design.
    (*ii*) Using the first specification, determine the zone in the time domain where

the closed-loop system response must lay. (iii) Recall that, according to Fig. 3.16, Chap. 3, the response of a second-order system remains between two exponential functions depending on ζ and ω_n. With this information and using the desired damping, determine the zone on the complex plane s where the dominant (complex conjugate) poles of the closed-loop system must be located. (iv) Use the root locus rules presented in this chapter to find the controller gains, ensuring that all the closed-loop poles are inside the desired zone in the plane s. (v) Verify that the second specification is satisfied and, if this is not the case, redesign the controller. (vi) Perform some simulations to corroborate that all the requirements are satisfied.

References

1. G. W. Evans, The story of Walter R. Evans and his textbook Control-Systems Dynamics, *IEEE Control Systems Magazine*, pp. 74–81, December 2004.
2. R. Kelly, V. Santibáñez, and A. Loría, *Control of robot manipulators in joint space*, Springer, London, 2005.
3. R. Kelly and V. Santibáñez, *Motion control of robot manipulators* (in Spanish), Pearson Prentice Hall, Madrid, 2003.
4. R. Kelly, PD control with desired gravity compensation of robotic manipulators: a review, *The International Journal of Robotics Research*, vo. 16, No. 5, pp. 660–672, 1997.
5. K. Ogata, *Modern control engineering*, 4th edition, Prentice-Hall, Upper Saddle River, 2002.
6. N. S. Nise, *Control systems engineering*, 5th edition, John Wiley and Sons, New Jersey, 2008.
7. R. C. Dorf and R. H. Bishop, *Modern control systems*, 10th edition, Pearson Prentice-Hall, 2005.
8. B. C. Kuo, *Automatic control systems*, Prentice-Hall, 1995.
9. G. H. Hostetter, C. J. Savant, and R. T. Stefani, *Design of feedback control systems*, Holt, Rinehart and Winston, 1982.
10. W. Ali and J. H. Burghart, Effects of lag controllers on the transient response, *IEE Proceedings-D, Control theory and applications*, vol. 138, no. 2, pp. 119–122, March 1991.